Journal of Engineering Mechanics and Machinery (2019) Vol. 4: 1-28 **DOI: 10.23977/jemm.2019.41001**
Clausius Scientific Press, Canada **ISSN 2371-9133**

'Butterfly acoustical skin' – new method of reducing aero acoustical noise for a quiet propeller

Igor S. Kovalev

Science and Technology Laboratory, Kinneret College, Emek Hayarden, 15132, Israel
Correspondence: kovis@ashdot-m.org.il

Keywords: 'butterfly acoustical skin', moth, noise reduction, porous scales, propeller.

Abstract: An experimental investigation was conducted on the effect 'butterfly acoustical skin' (metallic version of the lepidopterans scale coverage) on the acoustic performances of two - bladed propeller (diameter of 1200 mm, airfoil sections of NACA 2415, rotating speed of 1780 rpm, Re $\approx 2 \times 10^5$) in a low – speed straight through a wind tunnel. Attention was initially directed to this problem by observation of the porous scales and porous scale coverage of lepidopterans as well as other studies indicating the noise suppression of flying lepidopterans by wing appendages. The property of the moth coverage allows these insects to overcome bat attacks at night. These appendages are very small (size: 30 – 200 μm) and have a various porous structures. I discuss both many different micro – and nanostructures of the porous scales, and many differences in details among various structures of the porous scale coverage of lepidonterans. I consider here only porous scales of butterflies *Papilio nireus*, *Nieris rapae, Deelias nigrina*, male *Callophrys rubi*, male *Polyommatus daphnis*, butterfly *Papilio palinurus* as well as porous scale coverage of cabbage moth, moth of Saturniidae family and moth of *Noctuoidea* family. The evolutionary history of lepidopterans and the properties of lepidopterans scale coverage are briefly discussed as well as different methods of reducing aero acoustic noise of aircrafts.

The design of 'butterfly acoustical skin' with a hollow region imitates the cover hollow wing scale of the *Papilio nireus* butterfly. The design of 'butterfly acoustical skin' with a porous region imitates the cover hollow wing scale of the *Pieris rapae* butterfly, and from the cover hollow wing scale of the *Delieas nigrina* butterfly. Results indicate that the total sound pressure level of the rotating propeller with hollow skin is more than 2 dB lower with respect to the one with the smooth skin; and the total sound pressure level of the rotating propeller with the porous hollow skin is more than 4 dB lower with respect to the one with the smooth skin. The modification of acoustical effects on the rotating propeller with smooth 'butterfly acoustical skin' with a porous region was found to be to an acoustic absorption and to a dissipation of turbulent energy and to a reducing influence on noise generated. The same principles of the propeller noise reduction mechanism can explain by smooth 'butterfly acoustical skin' with a hollow region.

1. Introduction

Bio mimicry, sometimes called bionics, is the application of biological processes and forms found in nature to the study design of engineering systems [1]. For example, most owl species can approach their prey at the dead of night without being detected due to the uniqueness of their wings [2, 3]. The first report on the silent flight of owls, and description of the special adaptations of the owl feathers responsible for the quiet flight was given by Graham [4]. He identified three peculiarities of the owl feathers that are responsible for the quiet flight: the leading edge comb, the porous fringe on the trailing edge, and the downy upper surface of the feathers. The ability to fly silently has long been a source of inspiration for finding solution for quieter flight and fluid machinery. After more than a century the research regarding the mechanism that enables the nearly silent flight of owls remain an interesting field for theoretical and experimental research. Many of these mechanisms have already been tested for their applicability in technical airfoils, resulting for example in saw tooth [5] or serrated trailing edges [6], comb-like or brush-like flow-permeable trailing edges [7, 8] or porous airfoils [9]. These basic researches were often useful to design new axial fans which reduce noise emissions [10], design of future aircraft [11] and wind turbine blade [12].

1.1 Moths scale coverage vs. bats acoustic location

Bats and moths have been engaged in acoustic warfare for more than 60 million years. The interactions between bats and moths often been termed ‘an arms race’ (Figure 1). Moths and bats (order *Chiroptera*) are active by night. Most butterflies and moths live for just a few days and must evade predators and find food and a mate. Some moths use the method to reduce their conspicuousness (by the porous structure of scale coverage) to acoustic locating bats. Most *Chiropterans* orient in the environment, and capture prey in the dark with the use of acoustic location. There are two types of acoustic locations: the passive acoustic location which involves the detection of sound or vibration created by the insect being detected which is then analyzed to determine the location of the object; and active acoustic location which involves the creation of ultrasound in order to produce an echo, which is then analyzed to determine the size [13], the shape [14], and the texture [15] of the prey.

Noise and vibration in flying insects generally arise from two sources: the flapping wings and the oscillating sections of the thorax. These two sources far outweigh all other noise sources in flying insects. The observation that the noise of a flying insect is reduced by the moth scales was first measured by I.S. Kovalev [16]. He identified two peculiarities of the moth scale coverage that are responsible for the quiet flight: porous structure of wing appendages and porous structure of moth body coverage. The coverage and the scales convert the acoustic energy into heat. Moreover, laboratory experiments by I.S. Kovalev and A.K. Brodsky [17] showed that the presence of scales minimized the vibration of the flapping butterfly. Therefore the flapping flight of most moth species is silent and not audible to man and, more important, to their predators: bats and owls. In other words, the detection of flying moths by the passive acoustic location is difficult for predators.

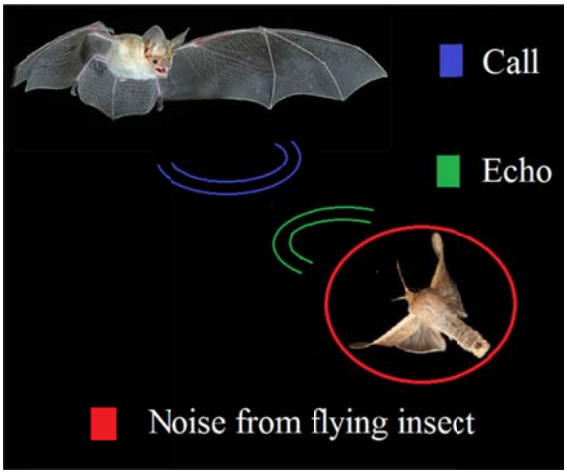

Figure 1 an acoustic warfare between moth and bat.

The active acoustic location is far more effective than the passive acoustic location. Typical FM bats make a series of very short chirps. The observation that the moth scale coverage insignificantly reduces the potential of the reflected ultrasound signal from a flying moth with bending wings was first measured by Roeder [18]. Kovalev's studies [19], Ntelezos's et al. studies [20], Zeng's et al. studies [21] as well as Shen's et al. studies [22] showed that the coverage of the flat plate wing absorbs more effective energy of an ultrasound signal than one of the bending wing [18]. When an ultrasound wave strikes the moth surface, part of bat's calls is transformed into heat in the scale coverage or transformed through thin layers of a wing chitin [19, 21 and 22], therefore the detection of the object (moth) by active acoustic location is difficult for the bat. This way, the property of the moth coverage allows the insect to overcome predator's attack at night. These facts motivated the work presented in this paper.

1.2 Porous scales and porous scale coverage of lepidopterans

Butterflies and moths both belong to the insect order *Lepidoptera*. These insects are usually called lepidopterans [23]. The world "*Lepidoptera*" is derived from the Greek word meaning "scale wing". The surface of the wings of these insects is covered with millions of tiny movable appendages – scales (30-200 m in size) [24] (Figure 2. a, b). These appendages are arranged in highly ordered rows in the same fashion as slate tiles on a roof. There are normally two types of chitinous scales tiled distally on each of the dorsal surfaces (also called upper wing surface) and ventral surfaces (also called lower wing surface) of *Lepidoptera* wings: the basal scales *Ba*, which lie directly above the wing lamina, and the cover scales *Co*, which overlay these [25].

The micro – and nanostructure of the *Lepidoptera* wing scales is a true miracle of nature. Each scale is attached to the wing membrane by short stalk *St* (Figure 2. c) and resembles dorsoventrally flattened sacs with an upper *UL* (also called obverse) and lower LL (also called reverse) lamina (Figure 2. d). The structure of the reverse lamina is generally undifferentiated. Both surfaces of the lamina are smooth, whereas the obverse lamina may possess an intricate architecture, typically composed of a series of longitudinal ridges *Lr*. Dorsal outgrowths of these, termed lamellae *L* (also called scutes), overlap anteriorly and may vary in the angle to which they are oriented with respect to the obverse lamina. Further outgrowths or flutes *Fl* are often located laterally on the ridges and may extend between them, forming cross ribs *Cr*. These scale structures (longitudinal ridges and cross ribs) produce a colorful iridescence from reflected sunlight [26]. Cross ribs *Cr* and longitudinal ridges frame open pores to the scale interior [25]. The average size of the open pores is 1 × 1μm; the obverse lamina has porosities from 40 to 50 percent. These structures are joined to the

reverse lamina by vertical supports or trabeculae *T* and the region between the trabeculae is termed the lumen *Lu*. The inverted V-profile of the longitudinal ridges form through micro pores, which are disposed between the rough upper lamina and smooth lower lamina. The average size of the through micro pores is from 1 to 1.5μm.

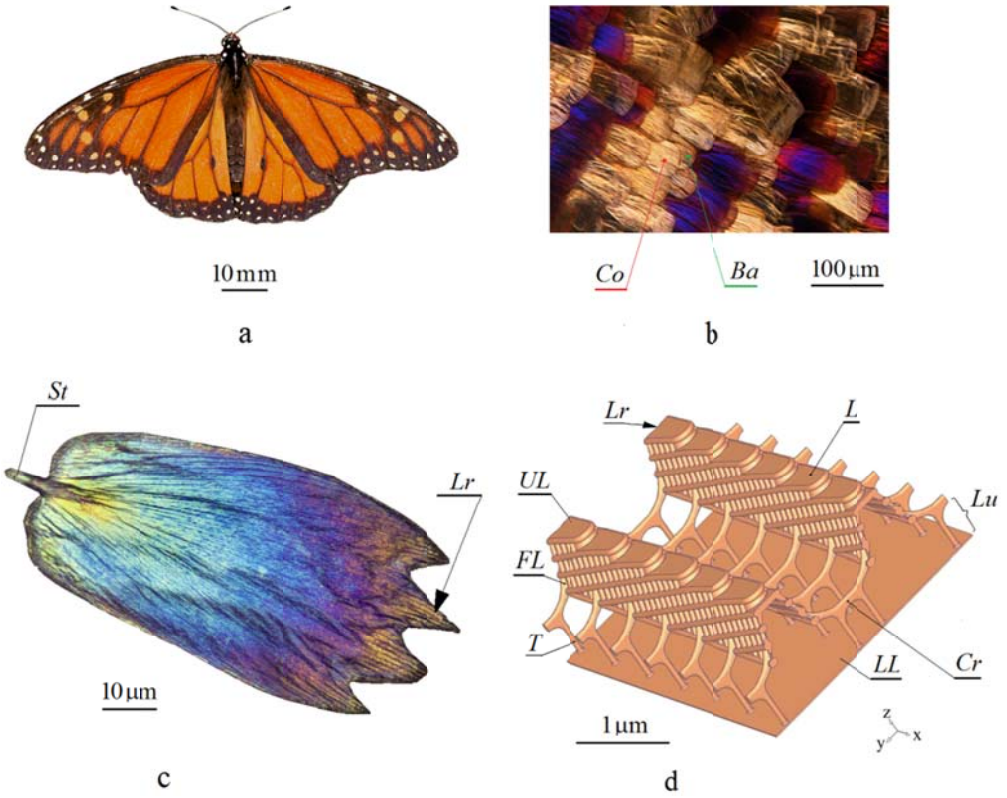

Figure 2 a. Dorsal wing surface of butterfly *Danaus plexippus*. b. Dorsal forewing of *MicroPterigoidea* moth showing cover scales (*Co*) overlaying basal scales (*Ba*). c. Hollow scale indicating the longitudinal ridges (*Lr*) and the short stalk (*St*). d. Nanostructure (vertical cross-section) of a cover hollow scale of butterfly *Danaus plexippus*, drawn in axonometric [27], where *UL* - upper lamina, *LL* – lower lamina, *L* – lamella, *Lu* – lumen, *Lr* - longitudinal ridges, *Cr* – cross rib, *Fl* – flute, *T* – trabecular.

This type of cover appendages is called porous scales [28 and 29] (also called hollow scales [30]). This construction of scales (Figure 2. d) is highly malleable, allowing extravagantly varying structures and shapes of the cover appendages, allowing many different micro – and nanostructures of scales to occur on lepidopterans wings. Actually, three types of porous scales of insect order *Lepidoptera* have been identified: mono-layered, double-layered and multi-layered. Mono-layered scales have only one porous layer – upper lamina plus solid lower lamina; double-layered scales have both porous layer and porous chitin structure PS plus solid lower lamina; multi-layered scales have three and more porous layers plus solid lower lamina (Figure 3).

First, I consider the mono-layered porous scales. The cover scales of the butterflies *Papilio nireus* (Figure 3. a, b) and *Danaus plexippus* (Figure 2. a, d) are mono-layered. The porous structure of *UL* of *Papilio nireus* scale has porosity values over 60 – 70 percent; the pore diameter is 240 nm (table), the scale thickness (without ridges *Lr*) is 3μm [31].

Next, I consider the double-layered porous scales. The cover scales of the butterflies *Callophrys rubi* (Figure 3.c), *Polyommatus daphnis* (Figure 3.e), *Delias nigrina* (Figure 3. h) and *Pieris rapae* (Figure 3. j) are double-layered. Porous chitin structure has been identified in the lumen of the butterfly *Callophrys rubi* (Figure 3. d) and the butterfly *Polyommatus daphnis* (Figure 3. f). This

type of porous structure is called 'cuticle crystal' [32]. The porous structure of *Callophrys rubi* scale has porosity values over 50-60 percent; the average diameter of the pores is 257±25 nm, the scale thickness (without ridges *Lr*) is 2µm [33]. The porosity of *Polyommatus daphnis* scale is high, with void volumes of 60-70 percent, and the largest pore diameters are about from 200 to 300 nm, the scale thickness (without ridges *Lr*) is 1.5µm. The micro – and nanostructure of upper lamina of these porous scales (Figure 3. d, f) is similar to the micro – and nanostructure of obverse lamina of the butterfly *Danaus plexippus* scales (Figure 2. d).

Another type of porous structure has been identified in the lumen of the butterfly *Delias nigrina* (Figure 3.g) and the butterfly *Pieris rapae* (Figure 3. i). The cover appendages of these butterflies are abundantly studded with micro beads (MB) (Figure 3. h and Figure 3. j) [34]. This type of PS has been classified as 'pigment granules' [34]. Every granule is elongated micro ovoid with dimensions of 100-500 nm [34]. The obverse lamina of *Delias nigrina* scale (Figure 3.h) has porosities from 40 to 50 per cent; the PS of these butterfly appendages has porosity values over 30-40 per cent, the scale thickness (without ridges *Lr*) is 1.5 m. The upper lamina of *Pieris rapae* (Figure 3.j) scale has porosities from 50 to 60 per cent; the porous structure of the scale has porosity values of over of 30-40 per cent, the scale thickness (without ridges) is 1.5µm.

Finally, I consider the multi-layered porous scales. The cover scales of the butterfly *Papilio palinurus* (Figure 3. l). *Papilio palinurus* appendage has 9 layers of cuticle scutes with air region. The cuticle lamella thickness is 102 nm; the air region thickness is 108 nm. The porous structure of *Papilio palinurus* scale has porosity values of over 50 – 60 percent; the average diameter of the pores is 175±25 nm [35].

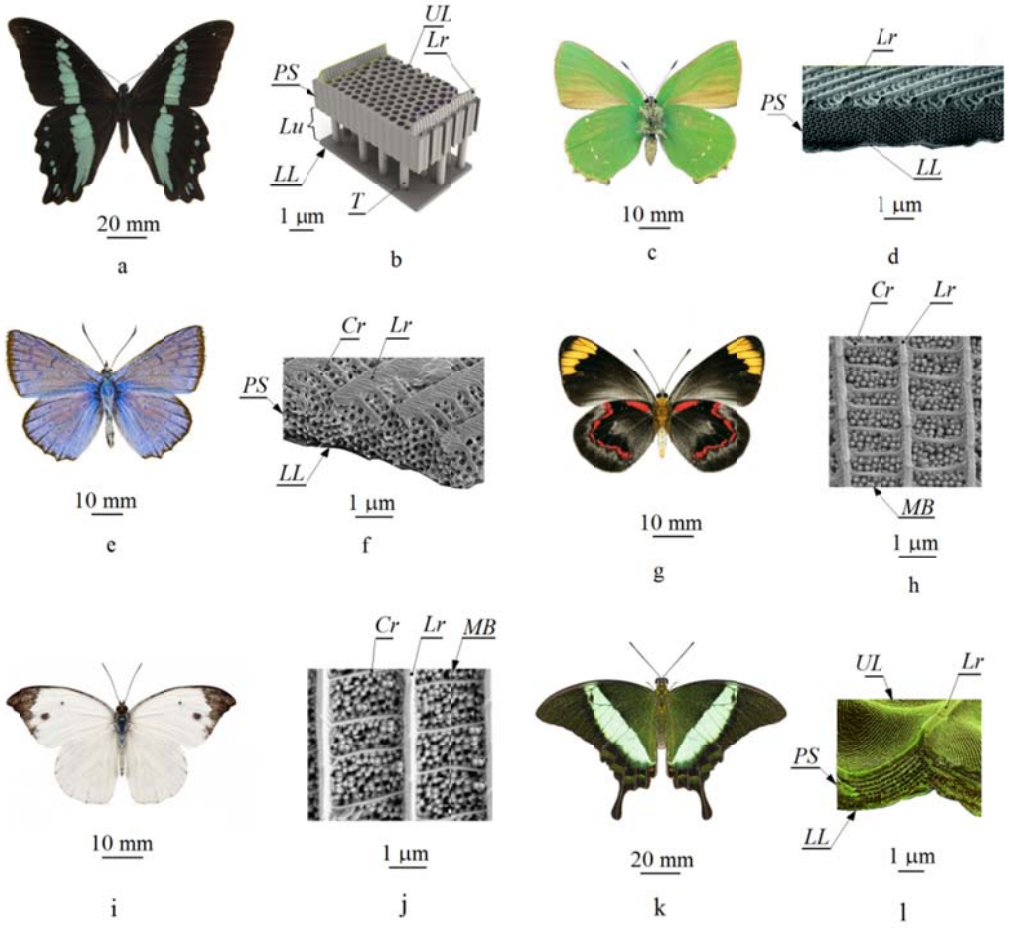

Figure 3 a. Dorsal wing surfaces of butterfly *Papilio nireus*. b. Nanostructure (vertical cross-section) of a cover porous scale of *Papilio nireus*, drawn in 30° isometric [31, 36]. c. Green ventral wing

surfaces of male *Callophrys rubi.* d. Scanning electron micrograph (SEM) showing a transverse view of a cover porous scale of *Callophrys rubi* [37] in axonometric plane. e. Dorsal wing surfaces of male *Polyommatus daphnis.* f. SEM showing a plan view of a cover porous scale of *Polyommatus daphnis* in axonometric plane [38]. g. Dorsal wing surfaces of butterfly *Delias nigrina*. h. SEM showing a plane view of cover porous scale of *Delias nigrina*. The scales are studded with pigment granules MB [34]. i. Ventral wing surfaces of butterfly *Pieris rapae*. j. SEM showing a plan view of cover porous scale from *Pieris rapae*. k. Dorsal wing surfaces of butterfly *Papilio palinurus.* l. SEM showing a transverse view of a cover porous scale of *Papilio palinurus* in axonometric plane. *Ps* – porous chitin structure, *Lr* - longitudinal ridges, *MB* – micro beads, *UL* - upper lamina, *LL* – lower lamina, *Lu* – lumen, *T* – trabecular.

Table 1 The porosities of the scales

Butterfly	**Type of porous scale**	**Porosity (%)**	**Porosity values (nm)**
Danaus plexippus	mono-layered	60-70*	240
Papilio nireus	mono-layered	60-70*	240
Callophrys rubi	double-layered	50-60**	257
Polyommatus daphnis	double-layered	60-70**	200-300
Delias nigrina	double-layered	30-40**	150-250
Pieris rapae	double-layered	30-40**	150-250
Papilio palinurus	multi-layered	50-60***	200-300

*- for *UL*, **- *for PS*, ***- for *UL* and *PS*.

On top of all this, there are normally two qualitatively different facing surfaces of the *Lepidoptera* porous scales: the rough porous surface, which has a high concentration of longitudinal ridges and of cross ribs on the obverse lamina, and the smooth porous surface, which has a low concentration of the fine micro – and nanostructures on the upper lamina [39]. For example, the facing surface of the porous scales of the butterfly *Papilio palinurus* (Figure 3. l) and butterfly *Papilio nireus* (Figure 3. b) is smooth; while the facing surface of the porous scales of the butterfly *Danaus plexippus* (Figure 2. d), butterfly *Callophrys rubi* (Figure 3. d, butterfly *Polyommatus daphnis* (Figure 3. f), butterfly *Delias nigrina* (Figure 3. h) and butterfly *Pieris rapae* (Figure 3. j) is rough. Moreover, the surfaces of the wings of the butterfly *Papilio ulyssesare* are covered with scales both with rough facing surface and with smooth facing surface [39].

In most butterflies there is one layer of these scales or two distinct layers on insect wings. As a rule, the scale coverage of the sub marginal area (wing tip) on moth wings is mono-layered, and one of the basal area (wing root) of the wings is multi-layered. The wing appendages of multi-layered coverage are separated by micro pores (also called scale clearances *SC* (Figure 4.b)). The moth scale coverage is more compound than the butterfly scale coverage. For example, the thickness of the scale coverage on a forewing of cabbage moth *Barathra Brassicae L.* [40] and the height of the scale clearance are decreased in direction from the basal area to the sub marginal area, and in direction from the costa (leading) edge to the trailing edge. In general, the scale clearance of the ventral surface of the wing is larger than the clear spacing of the dorsal surface (Figure 3.b) [41]. Moreover, the appendages coverage of the moth *Barathra Brassicae* wings has the surface density value of over 390-2600 scales per square millimeter. In the same way, wing appendages coverage of a moth has double porosity. On the one hand, the pores (scale clearance) are formed by scales (Figure 4.b); on the second hand, the pores are formed by the cross ribs and the longitudinal ridges on the upper lamina. On the whole, the scale coverage of lepidopterans can be classified as thin type

and as thick type. The first type of lepidopterans scale coverage is butterfly coverage; the second type is moth coverage.

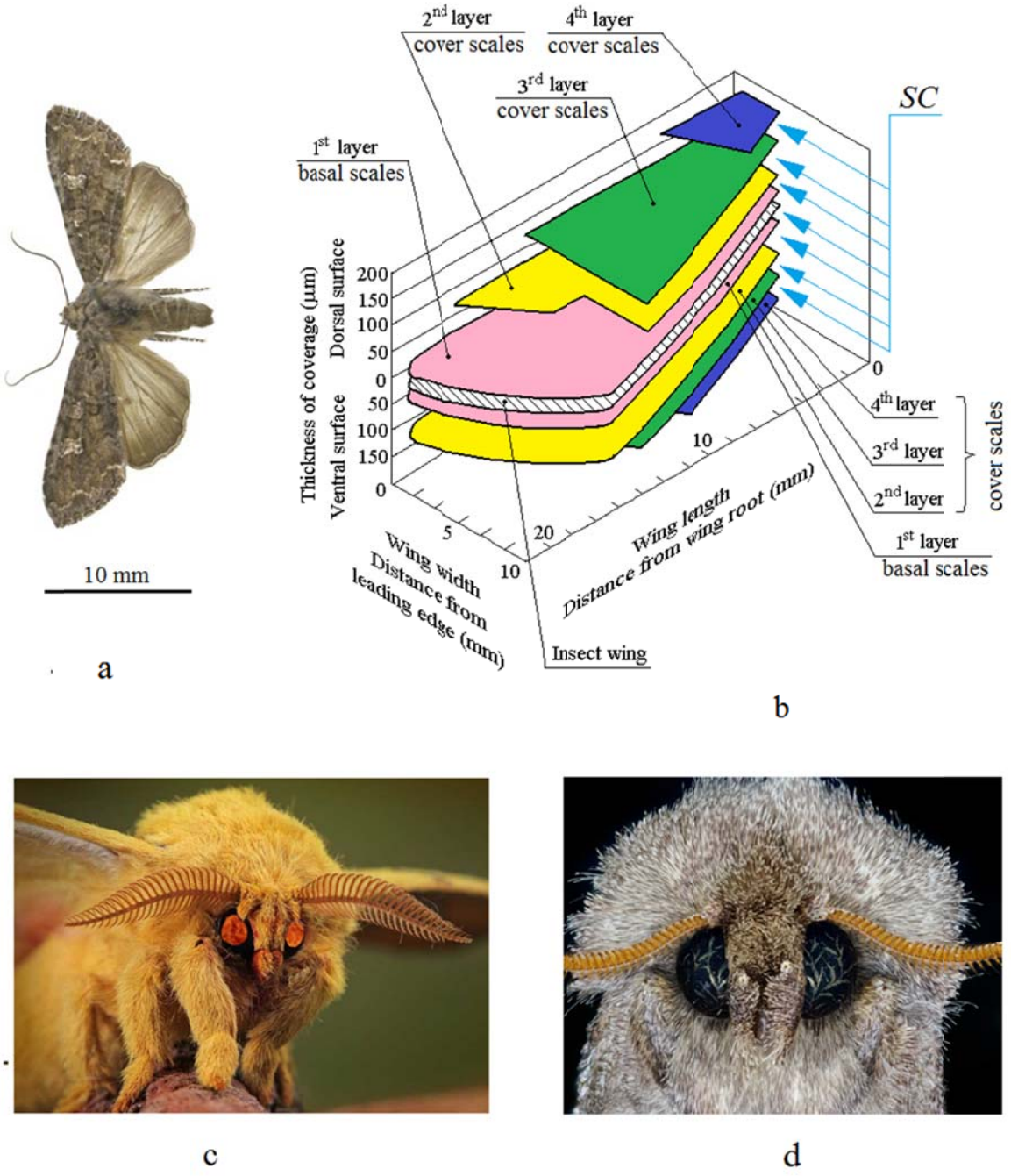

Figure 4 a. Dorsal wing surface of cabbage moth *Barathra Brassicae*. b. Structure of scale coverage on forewing of cabbage moth *Barathra Brassicae* (*SC* - scale clearance) [41], c. A moth of *Saturniidae* family, d. A front view of a moth's head (*Noctuoidea* family).

In contrast to the butterflies, all body parts (a head, a thorax and an abdomen) of the moths are covered with abundant appendages (scales and micro bristles) (Figure 4). The lepidopterans appendages, and accordingly, the scale clearances (which are formed by these appendages), can be arranged parallel to the body surfaces, at an inclination with respect to the body surfaces, and normal to these surfaces. For example, the wing scales of butterflies and the ones of the sub marginal area on moth wings are organized parallel to the wing surfaces (Figure 2. b and 4. b); the

appendages of a head, of a thorax and of an abdomen (*Saturniidae* family) are arranged at an inclination with respect to the body surfaces (Figure 4. c); the appendages of a head vertex, a frons and insect genae (*Noctuoidea* family) are organized normal to the surfaces (Figure 4. d).

1.3 An evolutionary history of lepidopterans and properties of lepidopterans scale coverage

There are some peculiarities with butterflies: they are the youngest insects in terms of their evolutionary history. The ancestors of present day butterflies flitted into air about 40-50 million years ago (the mid Eocene epoch) [42]. Moth evolved long before butterflies. *Archaelepis mane* is the earliest known lepidopteran fossil. It dates from the Lower Jurassic (ca 190 million years ago [43]).

Through natural selection, butterflies have been experimenting with scale microstructure and scale coverage for many million years. The scale microstructure and scale coverage of lepidopterans are multifunctional. Laboratory and nature examinations showed that the presence of the scales serve several functions: *(i)* increase the lift of wings of the nocturnal moth (*Catoealer*) [44], *(ii)* extend the movement capability of moth *Tinea tapotialla T.* [45], *(iii)* are involved in the process of temperature control of the body [46], *(iv)* confer some colors to lepidopterans [47]: mate color [48 and 49], warning color [50], camouflage color or mimicry [51], *(v)* absorb or reflect sunlight [52 and 53], *(vi)* generat sound [54] and (*vii*) protect insects from becoming ensnared in spider webs [55].

In addition, among all present day insects, lepidopterans with scale coverage are the record holders of two titles: long distance travel (butterfly *Danaus plexippus L.*) and flight speed (the flight speed of the moth *Agrotis ipsilo*was 113 km/h) [56].

We, thus, see that among lepidopterans, there are considerable differences in the micro – and nanostructure both of the porous scales and of the porous scales coverage. These can be correlated with the very different functions which these appendages serve.

1.4 Propeller

A propeller is a type of aeronautical propulsion system that transmits power by converting rotational motion into thrust. A history of aerodynamic propeller usually begins with mention of the Chinese flying top (ca. 400 B.C.) which was a stick with a propeller on top, which was spun by hands and released [57]. Among da Vinci's works (late 15th century) there were sketches of a machine for vertical flight using a screw-type propeller. The Wright brothers designed and tested aerodynamic propellers, and made the first powered flight in 1903 (Figure 5. a). Propellers were the first means of powering airplanes, preceding all other means of propulsion by about 40 years. Propellers were used extensively through 1940's. Although there have been many refinements to propellers through the years, the general appearance of the propellers has changed little (Figure 5). An aircraft propeller can be described as an open, rotating and bladed device [58]. Today, a renewed attention is being focused on the first aeronautical propulsion device - the propeller. This is due to the increased use of unmanned aerial vehicles [59], the growing market of general aviation, the increasing interest in ultra-light categories or light sport air vehicles, and the growing importance of environmental issues that have led to the development of all-electric emissionless aircrafts [59].

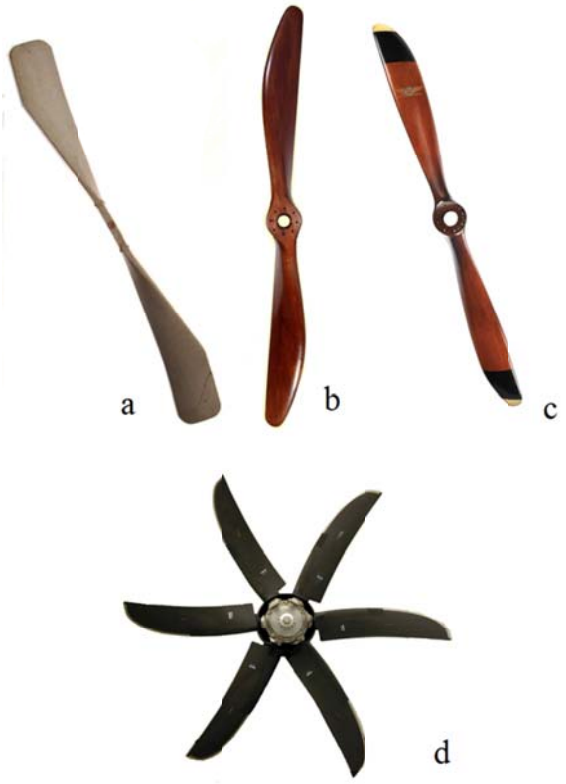

Figure 5 Wright brothers' propeller, b. Sopwith Camel propeller (1918), c. UWA – 0036 propeller (1943), d. Dowty R391 propeller (1996).

One of the most disturbing problems of propeller-driven aircraft was and still is their noise, which may limit the aircraft's operation. On the whole, the frequency range for human hearing, commonly referred to as audio frequencies, is typically cited as approximately 20 Hz - 20 KHz [60]. And while the human ear is sensitive to sounds between 0 and 140 dB, the sound level (140 dB) is too painful to the listener [61]. In propeller-based propulsion systems, the main sources of noise are the engine and the propeller. Propeller aircraft noise reduction has been studied since the early days of aviation. Initially the need for noise reduction was coupled with the need for reduced detectability in military operations [62]. Noise generated by aircrafts can propagate into the airport neighborhood and into the aircraft interior causing annoyance and discomfort of residents and passengers [63]. For example: the noise generated from the propeller of the aircraft XF 84 H was 135 dB and reportedly heard as far away as 40 km. This aircraft was not very popular with pilots. The propeller – driven strategic bomber Tu – 95 is considered to be the noisiest flying machine in current world aircraft. US submarines can detect the aircraft flying high overhead through their sonar domes while still underwater.

The acoustic signature of military aircraft has a significant effect on their detection. The importance of noise signature of propeller-driven air vehicles was already noticed during the 1960s [64]. Today, with the increased use of propeller-driven vehicles, there is a renewed interest in reducing the noise of propellers [65]. Many airports around the world impose strict limitations on noise level permitted during day or night.

The noise spectrum of a rotating propeller is caused by different sources and is usually classified in a broadband part and in a narrowband part (harmonic part or tonal noise). The broadband noise is generated by the rotating propeller due to all random aerodynamic behavior; more specifically it is the result of the propeller interaction with turbulence. It is usually distributed over a wide rage of frequencies and typically not periodic. The tonal noise is generated from the propeller blade airfoil

at a discrete frequency about 20 dB above the background broadband level. It is usually distributed over narrow range of frequencies and periodic. Many studies have been published on the characteristics and occurrence mechanisms of these noises [66, 67 and 68].

1.5 Methods of reducing aero acoustic noise

The noise of aircraft can be reduced by blade geometry modification of propeller, or by use porous sound-absorbing materials, also by porous media.

1.5.1 Blade geometry modification

Reducing the engine noise can be achieved by developing a suitable exhaust pipe or by using electric motors [69]. In the literature, three of the most prevalent methods of reducing aero acoustic noise (RAAN) from the propeller are presented. One of the most commonly known methods of RAAN is a blade geometry modification. It is well known, that different parameters in details among various designs, such as number of blades, blade shape, propeller diameter, blade pitch, trailing edge geometrical modifications and propeller blade fineness have impact on acoustic noise [70]. The propeller noise can be reduced by increasing blade sweep, reduction of blade thickness and reduction of tip speed [58].

1.5.2 Porous noise-absorbing materials

An alternative method of RAAN is made of a body material alteration. In most engineering constructions the bodies are made of rigid material. The aerodynamic surfaces of propeller driven aircraft are, traditionally, smooth and solid. If this material is replaced by a porous material, a reduction of the noise generated may be observed. In this context the term porous sound-absorbing material is applied to materials which have open and interconnected pores, so that air flow may enter through them. Porous sound-absorbing materials can be classified as cellular, fibrous or granular; this is based on their microscopic configurations. These materials can be formed by single grains, having solid structure, and by double porosity grains, having porous structure. Sound-absorbing materials absorb most of the sound energy striking them and reflect very little. The approach of porous material application for flow noise reduction was the subject to a number of studies in the past. Hayden R. and Chanaud [71] propose foil structures with reduced sound generation, claiming a considerable reduction of sound power levels for model scale airfoil. Some experimental studies conclude that fan noise can be reduced of 5 dB by the application of porous material blades [72 and 73]. Experiments on a model scale wing of a Lockheed L 1011 with flaps with porous surfaces have shown a noise reduction between 0 and 2 dB [74], depending on the parameters of the porous material used. For the reduction of rotor and turbo machinery noise for the vane leading edge the use of porous material was considered [75]. More recently, a number of numerical studies have focused on the application of porous material for slat trailing edges [76], on rotor trips [77], as well as turbo fan stator vanes [78].

While it is agreed that the application of porous materials may have an important potential for flow noise reduction [79 and 80], it is also stated that it is necessary to qualitative determine the effect of ‘butterfly acoustical skin’ on the rotating propeller acoustic.

1.5.3 Porous media

Porous media, such as screens and perforated plates, have been widely used in fluid dynamics studies since the 1940s [81]. These applications mostly occurred in the areas of

production/reduction of turbulence and the creation/elimination of large scale velocity or flow pressure. Important examples are the use of screens to minimize flow turbulence in wind tunnels [82], applications in boundary layer control [83] and reduction of aerodynamic forces.

1.5.3.1 Acoustic liner and micro perforated panel

Another method of RAAN to traditional sound absorbers made from porous materials is using acoustic liners (AL) (Figure 5. a) and micro perforated panels (MPP) (Figure 5. b). Liners (Figure 5. a) are applied on the internal walls of engine intakes and bypass ducts, in order to attenuate the fan noise while it propagates through the ducts before it is radiated to the exterior. The engine duct liners consists of a porous facing sheet (PFS) backed by a single layer of cellular separator such honeycomb cells (HC) with solid backing sheet (SBS). The acoustic performance of such liners is strongly dependent on the depth of the cell(s). Typical liner cell depth is from 38 mm to 76 mm; hole diameter is from 1 mm to 2.4 mm; face sheet thickness is from 0.5 mm to 1.0 mm, and percent open area is from 6.4% to 13.2% [84]. The fundamental absorbing mechanism of the AL is Helmholtz – resonance absorption. The MPP (Figure 5. b) has been introduced by D.-Y. Maa [85] and was devised to absorb sound, reducing its intensity. The MPP consists of porous facing sheet with air-back cavity (AC) and solid backing sheet. Typical MPP is from 0.5 mm to 2mm thick; the holes cover from 0.5% to 2% of the plate. Hole diameters are usually less than 1 mm, typically from 0.05 mm to 0.5 mm. The fundamental absorbing mechanism of the MPP is to convert acoustical energy into heat.

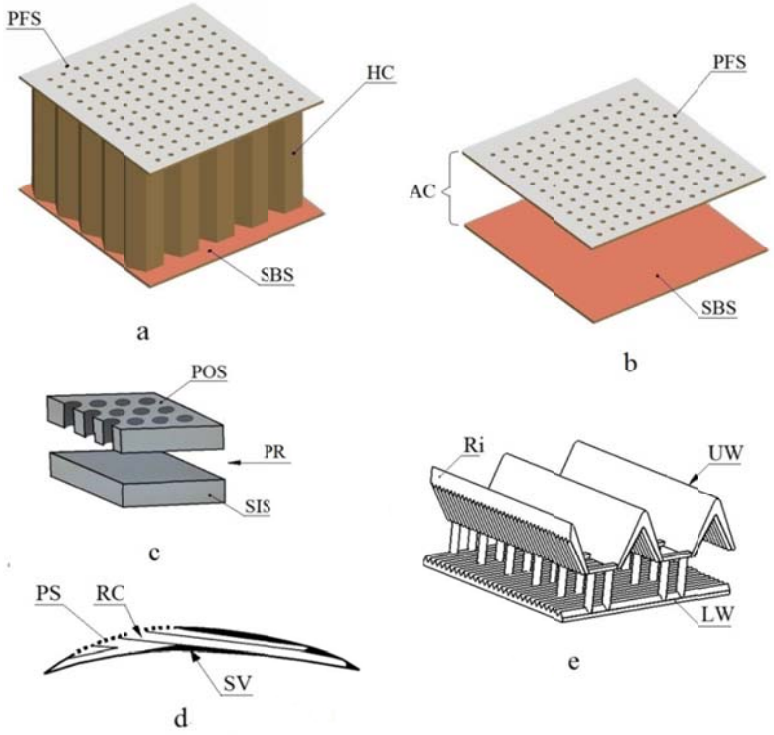

Figure 5. Porous medias

a. An acoustic liner, drawn in axonometric; b. A micro perforated panel, drawn in axonometric; c. Passive porosity, drawn in axonometric, d. Transverse view of soft vane configuration, e. Sketch of 'butterfly skin', drawn in axonometric.

POS – porous outer surface, PR – plenum region, SIS – solid inner surface, PS - porous surface, RC - resonant chambers, SV –soft vane, Ri - ridge, UW - upper metal, LW - lower metal wall; PFS - porous facing sheet; SBS -solid backing sheet; HC - honeycomb cells; AC - air cavity.

1.5.3.2 Passive porosity

In a later application, since the 1980s, the porous medium is in the form of a porous outer surface (POS), exposed to the flow at any given incidence. The system also includes a solid inner surface (SIS) such as the volume between the two forms of plenum region (PR) that is filled with the same fluid flowing over the outer surface [86]. This arrangement, known as passive porosity (Figure 5. c), redistributes pressure on the outer surface by establishing communication between regions of high and low pressure through the plenum. The pressure redistribution, which is associated with a minute transfer of mass into and out of the plenum, changes the effective aerodynamic shape of the outer surface. Typical hole diameter of passive porosity is around from 0.5 mm to 1.25 mm; skin thickness is around 0.5 mm; porosity is 22±10% (Figure 5. c). Passive porosity was used to reduce wave drag [87], and to reduce large side forces [88]. Passive porosity was also used to reduce the interaction noise in turbo machinery, for example, the noise reduction of a stator vane by passive porosity was 2.5 dB [78].

1.5.3.3 Soft vane

Another aircraft noise reduction concept was developed by NASA over the last ten years [89]. This concept is the soft vane, wherein a portion of the fan exit guide vane surface is made porous to allow communication between pressure fluctuations at the vane surface and multiple, internal resonant chambers or Helmholtz resonators (the internal chambers are skewed (not perpendicular to the porous surface) (Figure 5. d)). The arrangement provides acoustic absorption by inducing viscous dissipation at internal solid structure surface. For soft vanes, approximately 2 dB noise reduction was achieved [89]. The hole diameter of perforated sheet is around 0.635 mm; face sheet thickness is around 0.635 mm and porosity is 15 per cents.

1.6 'Butterfly skin'

Experimental investigations of the wing skin, called 'butterfly skin' (metallic version of the butterfly scale) (Figure 5. e) showed that this skin modified the effects and the vibration performance on the airfoil. On the one hand, 'butterfly skin' increased the lift force. On the other hand, the wing skin reduced the vibration duration and the frequency of an oscillation airfoil [27 and 41]. The 'butterfly skin' imitated the hollow wing scale (Figure 2. d). This skin was 333 times life size (the thickness was 1 mm) (Figure 5. e). 'Butterfly skin' was composed by two layers. The upper metal wall *UW* and the lower metal wall *LW* were separated by an air cavity (0.4 – 0.7 mm in clear spacing). Both sides of the upper wall were covered with a large number of span wise grooves. The depth of each groove was 0.5 mm. The ridges *Ri* (spacing 1 mm) with an inverted V-profile were formed between grooves. The grooves of the external surface were provided with lines of perforations (each opening was 0.4 mm × 0.4 mm in size). The inverted V-profile of the ridges formed the channels, which were disposed between the upper metal wall and lower wall. The lower metal wall was similar to a thin sheet. The internal surfaces of the recesses were covered with a large number of micro corrugations, which were perpendicular to the ridges *Ri*, and to the flow of surrounding air 1. The depth of each corrugation was 0.05 mm [90].

The principal concern of this study is to determine the effect of 'butterfly acoustical skin' (metallic version of the lepidopterans porous scale) on the acoustic performances of two-bladed propeller.

2. Material and experimental methods.

2.1 Wind-tunnel

The aero acoustic features of low-speed propellers were tested in the Zaporozhe Machine-Building Design Bureau (ZMBDB) low speed straight through a wind-tunnel (Figure 6). Air was driven from a high pressure storage *HPS* through the valve *Va* into a wide chamber *WC* with a low velocity. A screen *S* of wire gauze helped to equalize the velocity, across the cross-section of the chamber. A honeycomb *H* ensured that there was no large-scale swirling around in the channel, and that the air traveled along it in straight lines. The irregularity of wind of the wide chamber was swamped by the large space. Thus a uniform increase in velocity that occurred when the air passed through the narrower nozzle *N* (diameter of 2000 mm) was attained. A contraction section of the nozzle was designed using a matched pair of cubic curves. Thus, the airstream in the working section was uniform (the drift of the free stream velocity was less than about 0.9%) and laminar (the free stream turbulence level was less than 0.5% of the free stream velocity). The air speed of the wind tunnel was 30 m/s. One typical Reynolds based on chord length on this wind speed was 200000.

Test section winds were measured using a Pitot-static tube connected to a Datametric Barocel Electronic Manometer. Pressure differences down to 0.0001 in H_2O could then be measured. Turbulent velocity data and mean speed were also measured by using a constant temperature hot-wire anemometer. Air temperature was maintained at 20˚C.

All aero acoustic tests were carried out on two bladed propellers in the square anechoic room (length was 6 m, width was 4 m, and the height was 3 m) lined with absorptive acoustic wedges. Room location was at the Research Center of ZMBDB. The energy cut-off of the anechoic wedges had a sound absorption coefficient at normal incidence greater than 0.99. The collector was downstream of the test section. Noise-absorbing furry materials were attached to the surface of the collector to reduce the interaction noise between the open jet and the collector. The background noise was about 34 dB at a free stream velocity of 30.0 m/s. Figure 6 shows a picture of the chamber and a sketch of the layout of the experimental setup.

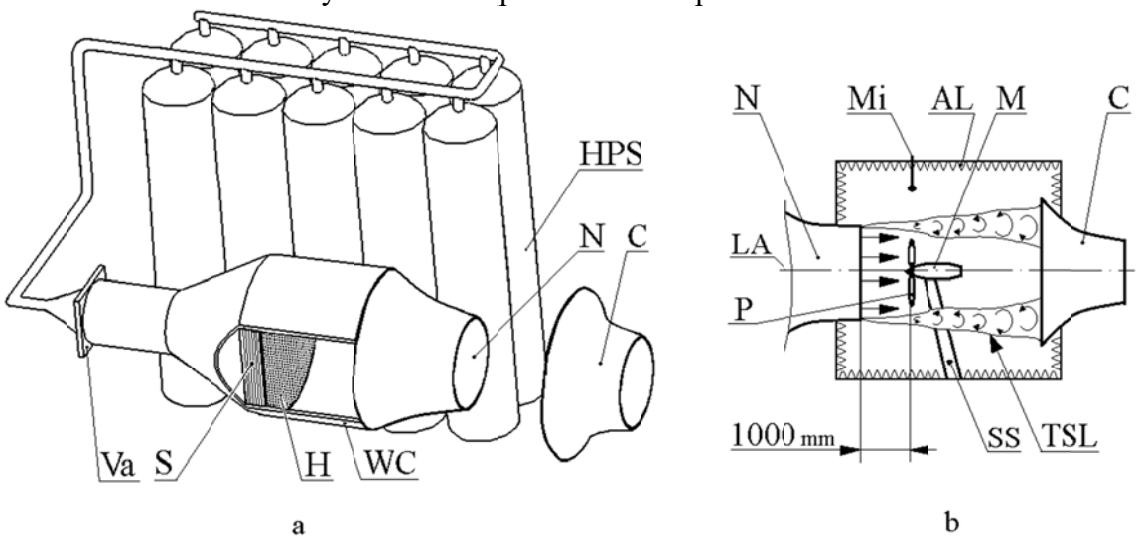

Figure 6 Scheme of the ZMBDB wind tunnel.

a. Axonometric view of the ZMBDB wind tunnel, b. Transverse view (along the longitudinal axis *LA*) of experimental apparatus installed in the ZMBDB wind tunnel open test section.

AL – Acoustic lining, *P* – propeller; *Mi* –microphone; M – motor; *C* – collector; *H* - honeycomb flow straightened; *HPS* - high pressure storage; *N* - nozzle; *S* – screen; *Va* – valve; *WC* - wide chamber, *TSL* - turbulent shear layer, *SS* - supporting strut, *LA* - longitudinal axis of the wind-tunnel.

The measurements of noise were made during the evolution of the low-speed propellers in the square anechoic room. The acoustic instruments were produced by Brüel and Kjær and consisted in a sound and vibration analyzer Pulse-X3570 integrated with FFT and CPB analysis tools, a Nexus 2690 amplifier and 1 free field ¼" microphones type 4939 with a dynamic range of 28 Hz to 164 kHz, 200 V polarization. The sensitivity calibrated at 250 Hz by using piston phone type 4228 with ¼" adaptor DP 0775. The narrowband sound pressure level spectra were computed with a Fast Fourier Transform size of 8192, giving a frequency resolution of 0.2 Hz. The sampling frequency of acoustic instruments spans from 0.026 Hz to 28 Hz, depending on the maximum frequency to measure, and on the number of lines of discretization. In these measurements I have adopted a resolution in the range 0.026 – 0.25 Hz, which guarantees a quite sharp definition of the acoustic discrete tones. The temperature and humidity inside the anechoic room were recorded to enable computation of the atmospheric absorption. The sound pressure levels (SPL) spectra were corrected for actuator response free-field correction, and atmospheric absorption. The overall sound pressure level (OSPL) was calculated through integration of SPL spectrum.

Previous theoretical predictions [91 and 92] and experimental researches [93] showed that, when the observer/microphone moved from the axial location toward the rotation plane, the harmonic contribution of propeller noise became more evident, while the broadband term decreased, and then eventually the harmonic contribution dominated over the other contributions in proximity of the rotational plane. Following these conclusions, the microphone was attached *to the* anechoic *room ceiling* and lay *in the intersection of two planes:* the rotation plane and the vertical plane along the longitudinal axis of the wind-tunnel. The sensor was placed out of the air stream one diameter from the center of the propeller rotation, and the microphone locations were outside of the turbulent shear layer *TSL*. The position of the microphone relative to the propeller is shown in Figure 6.

The propellers were driven by an electro motor M, which provided a power of 102 kW at a rotational speed of 1780 revolutions per minute (rpm). The motor pylon was mounted to an aerodynamically shaped strut SS which was securely anchored to the floor by means of steel tracks embedded into it (the floor and the supporting strut were then covered with acoustic foams). Power was supplied by a 240 V three-phase electrical bus and controlled from the observation room. This allowed the experimenter to operate both the data acquisition software and experimental apparatus from one location set in an adjacent room where a designated control desk was set. The motor controller of choice was selected due to its external display (indicating motor rotational speed) and compatibility with an external potentiometer used to finely adjusts the motor's revolutions per minute. In order to mount the propellers on the shaft of the motor, an aluminum adapter was produced, to ensure that the ambient noise, which also includes the noise from the electrical motor itself, is not excessively high. The total sound pressure level of the motor was 39 dB at a free stream velocity of 30.0 m/s. A set of measurements was taken with the free electrical motor alone, and it was found that for rotational speeds exceeding 1780 rpm the background noise was small.

2.2 Propellers

Three different propellers were used (Figure 7. a, b and c). The skin of first propeller (Figure 7. a) imitated the cover hollow wing scale of the *Papilio nireus* butterfly (Figure 3. b). This skin called smooth butterfly skin with a hollow region (SBSwHR) (Figure 7. a) was 400 times life size (the thickness was 1.2 mm) (Figure 7. a, b). SBSwHR was composed of two layers. The upper metal wall UW (the thickness was 0.5 mm) and the lower metal wall LW (the thickness was 0.2 mm) were separated by an air cavity AC (0.5 mm in clear spacing) Figure 7. d). Both metal layers were joined by vertical supports VS. The facing surface and opposite side of the UW were smooth. The external wall (UW) provided with diagonally staggered rows of round perforation (hole diameter was 0.5 mm). The porosity of the UW was 40 percent. This metal wall was manufactured by ANDRITZ Fiedler Company. The lower metal wall LW was similar to a thin sheet. Since, the propeller blade shape was very complex and different, the blade was made with eleven butterfly skin segments: $S_1, S_2, S_3,\ldots, S_{11}$ (Figure 7. a). The butterfly skin segments were formed around the blade. Initially, every segment was supported by the propeller body and was affixed on the smooth outer surface of the propeller blade. Then, the segments were disposed very close to each other (Figure 7. g). Finally, every abutment joint (AJ) was covered with glue putty (GP) and was formed a flush joint (FJ) (Figure7. h). The structural design of the SBSwHR is similar both to one of the micro perforated panel (Figure 5. b) and to one of the passive porosity (Figure 5. c).

The skin of the second propeller imitated the cover porous wing scale of the *Pieris rapae* butterfly (Figure 3. j) and the cover porous wing scale of the *Delias nigrina* butterfly (Figure 3. h). This skin called smooth butterfly skin with a porous region (SBSwPR) (Figure 7. b) was 800 times life size (the thickness was 1.2 mm) (Figure 7). SBSwPR was composed of free layers (Figure 7). The experimental studies by Pechan and Sencu [94] and by Hamacawa et al. [95] showed that various surface imperfections (groove, ridge and et cetera) of the propeller blade [94] or of the airfoil [95] may generate the noise. So, the faicing surface and opposite side of UW were smoth. The upper metal wall UW of the SBSwPR was geometrically similar to the UW of the SBSwHR. The lower metal wall LW was similar to a thin sheet.

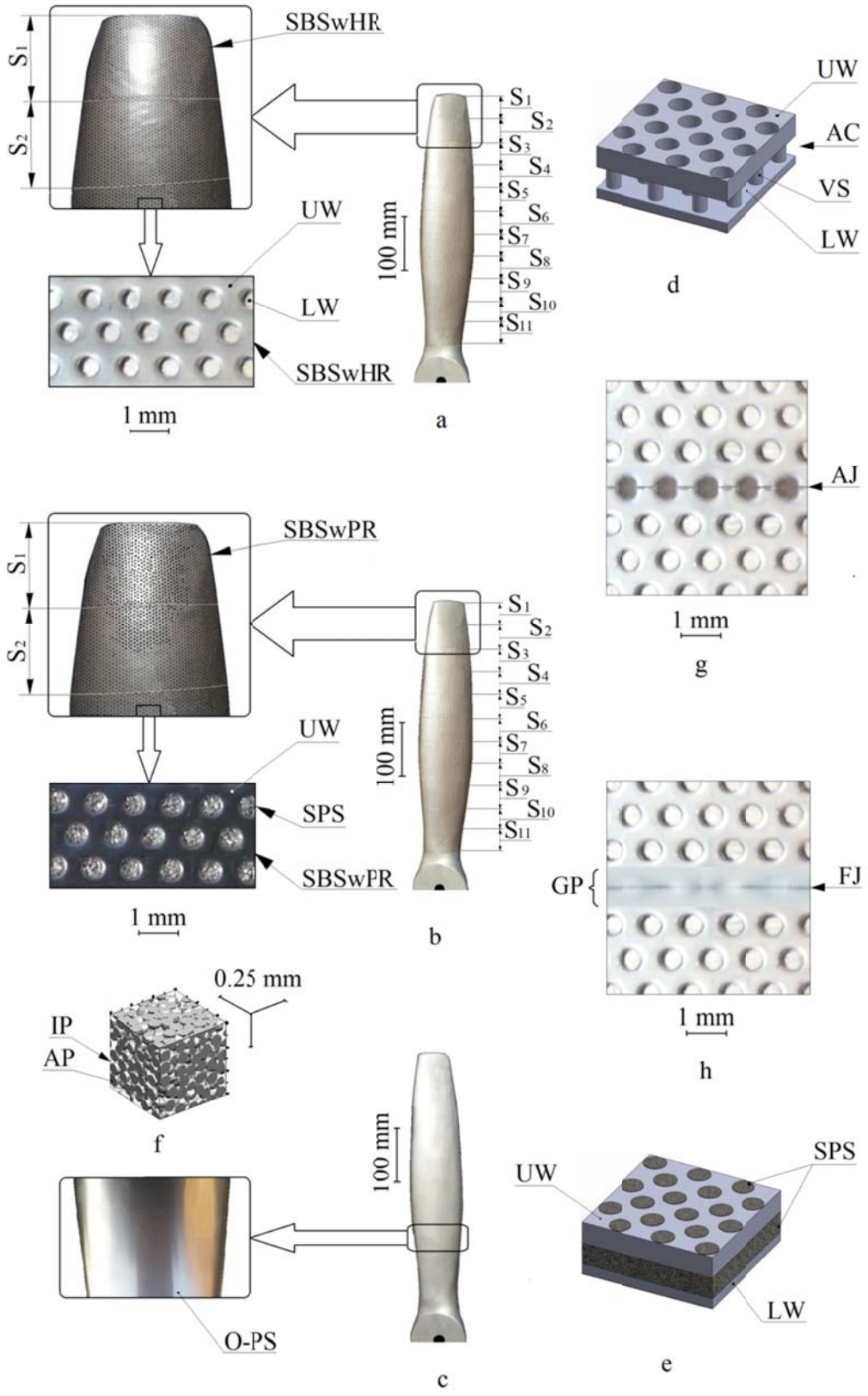

Figure 7. Front view of three propellers.
a. propeller with SBSwHR, b. propeller with SBSwPR, c. propeller with one-piece skin, d. a vertical cross-section of the smooth butterfly skin with a hollow region in axonometric plane, e. a

vertical cross-section of the smooth butterfly skin with a porous region in axonometric plane, f. 3D computer tomography of the sintered powder stuffing in axonometric plane, g. fragment from adjoining segments of SBSwHR with matched joint, h. fragment from adjoining segments of SBSwHR with putty flush joint.
SBSwHR - smooth butterfly skin with a hollow region, $S_1, S_2, S_3,\ldots, S_{11}$ - butterfly skin segments, UW - upper metal wall, AC - air cavity, VS - vertical support, LW - lower metal wall, SPS - sintered powder stuffing, SBSwPR - smooth butterfly skin with a porous region, AP - aluminum powder, IP - inter particle porosity, O-PS - one-piece skin, AJ - abutment joint, GP - glue putty, FJ - flush joint.

The air hole between UW and LW and the round hole perforations of the UW were filled with porosity material. The sintered powder stuffing SPS was manufactured by ZMBDB. The thickness of the UW was 0.5 mm, the thickness of the SPS was 0.5 mm and thickness of the LW was 0.2 mm. The aluminum powder AP sizes were in the range of 50 to 65 μm, and inter particle porosity IP was 35 per cent (Figure 7. f). The facing surface of the UW was disposed flush the exterior surface of the powder stuffing (Figure 7. l). The sintered production process is described in detail in work [96]. A brief description of this process is submitted follows. Initially a hydraulic press, cold-molding die was made. Then, an aluminum powder with an incorporated amount phenolic binder was poured into the die. Next, the die assembly was jogged to settle the powder, and baked at 230° C to cure the phenolic binder. Finally, the stuffing was removed from the die in the molded-and-cured form ready for sintering. The stuffing was sintered at 560° C for four hours in vacuum of 1×10^{-6} to 1×10^{-7} Torr. This sintered process used the aluminum powders, which were manufactured by Valimet Inc. Similar to the first propeller which the SBSwHS, the blade of second propeller was made with eleven segments of the SBSwPR (Figure 7. b). Similarity these butterfly skin segments were formed around the blade, and as well each segment affixed on the smooth outer surface of the second propeller blade, and were disposed very close to each other, and formed a putty flush joint. For the structural design of the SBSwPR there are not equivalents in the modern porous media.

Since the SBSwHR and the SBSwPR imitated the cover wing scales of one order – *Lepidoptera*, so I incorporated both these skins (SBSwHR and SBSwPR) into one group – 'butterfly acoustical skin' - BAS.

It is the principal concern of this study to qualitatively determine the effect of butterfly skin on the rotating propeller acoustic. Therefore, the metal skin (O-PS) of the third propeller was one-piece, smooth and airproof. The skin thickness was 1.2 mm. The blades of the third propeller were hand-finished (Figure 7.c) to highly smooth and polished surfaces, using 12000 - grit sand paper. The skin was chaped around the blade, and was affixed on the smooth outer surface of the third propeller blade. All the three propellers had identical geometric parameters: airfoil sections (NACA 2415), diameter (1200 mm), thickness, chord and pitch. The acoustical properties of the third propeller were compared with that of the first and second propellers.

3. Results

This section presents the acoustic results for the three propellers. The discussion focuses on the blade passing frequency (BPF) tones of these propellers. Figure 8. a, b and c corresponding to the blade skin displayed in Figure. 8 for rotational speed 1780 rpm. The frequency along the horizontal axis ranges from 0 to 3,800 Hz, covering both the narrowband and the broadband parts of the total noise. The harmonic part is shown in the lower frequency range (e. g. from 0 to approximately 3,250 Hz for smooth skin in Figure 8. a, and from 0 to approximately 2,200 Hz for hollow skin in Figure 8. b). The tonal noise levels represent most of the contribution to the total noise (Figure 8. a and b), while the broadband noise represents only a small portion.

Initially, I examined the smooth rotating propeller acoustics. Figure 8.a displays the near field narrowband SPS spectra in the rotor plane. In this plane the fundamental BPF ton 1 and its higher harmonics up to tone 6 is dominant. The peak of the tone 1 is 25 dB above the broadband noise. Figure 8. a shows that rotating propeller generated tones at harmonics of 567 Hz at high levels over 65 dB extending from low frequencies to approximately 2,700 Hz. These rotating propeller tones begin at 82.6 dB and drop to approximately 63 dB at 3,250 Hz. The total sound pressure level OSPL of the rotating propeller with the smooth skin, which takes into account the entire frequency domain (0…100 kHz), is 56.5 dB.

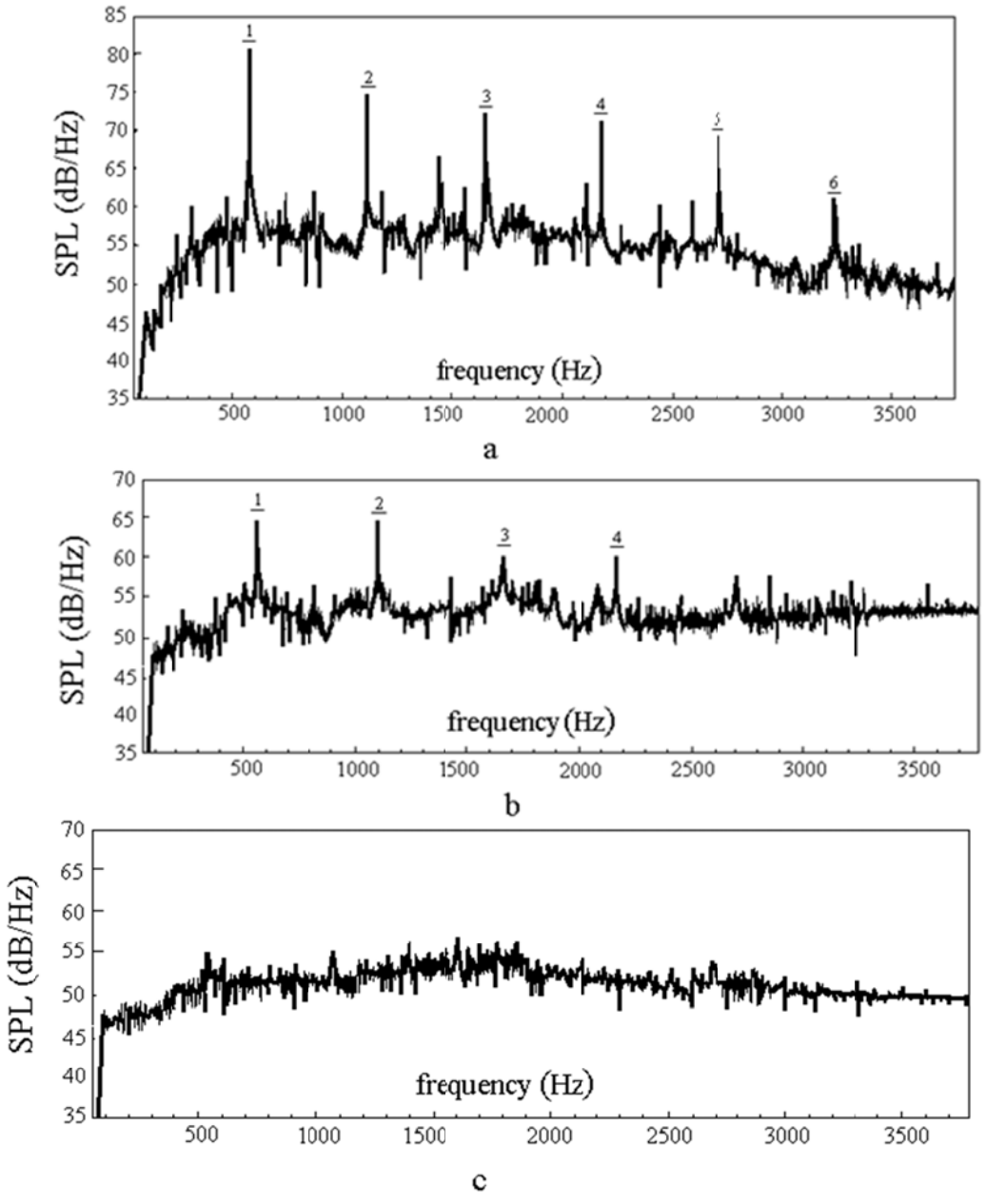

Figure 8 Near field SPL spectra for the rotating propeller with smooth skin (a), hollow skin (b) and porous hollow skin (c).

Then, I examine the impact of the hollow skin on rotating propeller acoustics. Figure 8. b plots the near field noise narrow band and broadband SPL spectra from rotating propeller with the hollow skin in the rotor plane. Multiple peaks are observed on the spectrum. Examining the spectrum I

clearly distinguish tones 1, 2, 3 and 4. I observe a temperate content of tones, with the principal ones labeled. The fundamental BPF tones 1 and 2 are dominant and have similar magnitude. The next stronger tones 3 and 4 are about 3 dB lower than the dominant tones. Higher harmonics 5 and 6 are buried in the broadband noise. The maximum peak level of the spectrum is approximately 18.6 dB lower than the higher harmonic 1 of the propeller with the smooth skin at 567 Hz. Therefore, this skin is effective to reduce the tonal noise from the rotating propeller. On the other hand, the broad band noise is slightly increased from 2,300 Hz to 3,800 Hz for the rotating propeller with hollow skin (Figure 8. b). One of the main mechanisms of generating higher amplitude broad band noise is the turbulent boundary layer flow developing over the porous outer surface of the hollow skin. The skin increases the velocity disturbance in the boundary layer on the porous outer surface of the rotating propeller, and increases the turbulent noise [97]. The total sound pressure level OSPL of the rotating propeller with the hollow skin, is 54.2 dB. A quantitative comparison of the sound pressure levels shows that the total sound level of the rotating propeller with the hollow skin is more than 2 dB lower with respect to the one with the smooth skin. This result compares well with the noise reduction of a stator vane by passive porosity [80].

Finally, I examine the impact of the porous hollow skin on the rotating propeller acoustics. Figure 8. c displays the near field noise from rotating propeller with the porous hollow skin in the rotor plane. No peaks are formed in the spectra – all harmonics are buried in the broadband noise. The broad band part dominates over the other contributions in the rotor plane. Based on the spectra results (Figure 8. c), it seems that the most effective mechanism of reducing the acoustic waves in the harmonic part of the noise spectrum is the rotating propeller with the porous hollow skin. Moreover, Figure 8. c shows a slight decrease in the broad band noise level from 2,300 Hz to 3,800 Hz for the propeller. It is clear that the porous hollow skin is more efficient in reducing broadband noise than the hollow skin. This suggests that the porous diameter of the porous hollow skin (0.1 mm) is less efficient in exciting the turbulent noise than the one of the hollow skin (0.5 mm). The total sound pressure level OSPL of the rotating propeller with the porous hollow skin, is 52.5 dB. A quantitative comparison of the sound pressure levels shows that the total sound pressure level of the rotating propeller with the porous hollow skin is more than 1.5 dB lower with respect to the one with the hollow skin and is more than 4 dB lower with respect to the one with the smooth skin. The latter result compares well with the noise reduction of the porous-bladed fan given by Chanaud at al [75].

4. Discussion

4.1. Propeller noise reduction

The major propeller noise components are thickness noise (due to the volume displacement of the blades), steady-loading noise (due to the steady forces on the blades), unsteady-loading noise (due to circumferentially nonuniform loading), quadrupole (nonlinear) noise, and broadband noise [68]. Each one of these components acts on the blade surfaces.

4.1.1 Noise absorption mechanism of propeller with SBSwPR

Sarradj E. and Geyer [97] showed the noise reduction mechanism by porous airfoils. I developed the mechanism of propeller noise reduction by SBSwPR on the basis of Sarradj's and Geyer's mechanism. Noise absorption of a propeller with SBSwPR follows three aspects. The first of these aspects is acoustic absorption. Sintered powder stuffing of SBSwPR contains through pores and micro channels so that sound waves are able to easly enter through them. When sound enters the stuffing, owing to sound pressure, air molecules oscillate in the interconnecting voids that separate

the micro granules with the frequency of the exiting sound wave. This oscillation results in frictional losses. A change in the flow direction of sound waves, together with the expansion and contraction phenomenon of flow through irregular pores, results in a loss of momentum. Owing to the exciting of sound, air molecules in the pores undergo periodic compression and relaxation. This results in change of temperature. Because of long time, large surface to volume ratios and high heat conductivity of powder stuffing, heat exchange takes place isothermally at low frequencies. At the same time in the high frequency region compression takes place adiabatically. In the frequency region between these isothermal and adiabatic compression, the heat exchange results in loss of sound energy. So, the reasons for the acoustic energy loss when sound passes through sound absorbing materials are due to: frictional losses, momentum losses and temperature fluctuations [98 and 99]. Another possible aspect is the dissipation of turbulent energy from boundary layer by the porous surface. This would also result in less broad band noise generation at the trailing edge. The third aspect is the reducing influence on noise generated by the contact of turbulence with leading edge and also on other noise generation components. In addition, scattering of the micro granules also influences the absorption of sound energy inside the powder stuffing.

4.1.1 Propeller noise reduction mechanism by SBSwHR

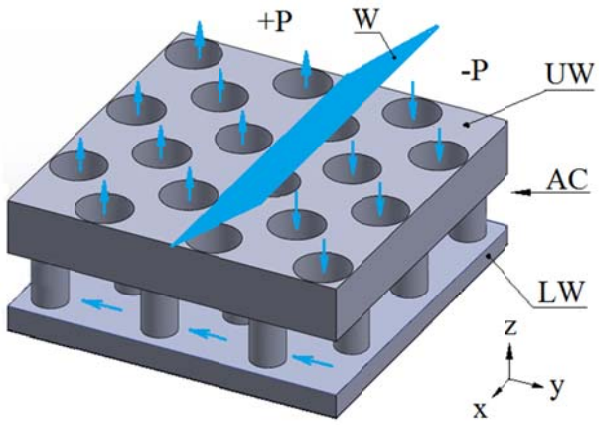

Figure: 9 The influence of the sound wave W on the SBSwHR, drawn in axonometric.

AC – air cavity; W - sound wave, UW – upper wall, LW – lower wall, +P – high pressure region, -P – low pressure region.

It is well known, that fan noise reduction can be achieved either by design aiming for it at the source or by incorporating acoustic treatment to absorb the noise produced by the source [78]. Approaches to reduce noise at the source are based on the fact that any of the significant noise generating mechanisms is related to unsteady, periodic forces acting on the surfaces of rotating fan, and caused by gust-type disturbances. These unsteady forces give rise to acoustic perturbations that propagate through the fan duct and radiate as noise. The noise level generated from this source is directly proportional to the magnitude of the fluctuating lift force. Thus, any reduction in this fluctuating force would result in a reduction in noise.

Tinetty A.F. et al. [78] shows the mechanism to reduce interaction noise in turbo machinery by passive porosity on the stator vane. I developed the mechanism of a propeller noise reduction by SBSwHR on the basis of Tinetty's mechanism. Figure 9 shows a schematical drawing of what may be assumed to happen. In Figure 9 I plotted a local sound wave W in (Y-Z-X) plane around a fragment of SBSwHR in an axonometric view. A rotating propeller produces unsteady and periodic forces acting on the porous outer surface of SBSwHR, which result in sound wave radiation. The sound wave produces the high – pressure region +P and the low – pressure region –P on the upper

wall (UW). The regions with a pressure difference are connected by porous of the UW and by the air cavity AC. Therefore, the air is transferred through the AC in a direction from the high – pressure region +P to the low-pressure region -P. Thus, the pressure difference between the two regions is redistributed and is reduced. For this reason the propeller noise is decreased.

4.2. Suggestions for further research of 'butterfly acoustical skin'

There is no doubt that nature is not a constructor in the sense that an engineer is. In the last resort it is inimitable. Even so, the engineer should venture a glance at biological structures of the butterfly scale, he will hardly find a readymade solution of his own technical problems but he may expect a variety of interesting hints.

Based on the method of noise reducing of lepidopterans both by the porous structure of wing appendages and by the porous structure of the moth body coverage, which evolved for many million years through a natural selection, I present both the future of propeller design with different designs of 'butterfly acoustical skin' which reduce noise emission, and the classification of the skin.

By analogy with the scale coverage of lepidopterans, 'butterfly acoustical skin' (BAS) could be classified as thin type (thin BAS) and thick type (thick BAS). The first type of 'butterfly acoustical skin' is formed around the propeller blade PB and is affixed on the outer propeller surface (Figure 10.a, b and c). Moreover, by analogy with the scale coverage of lepidopterans, the structure of the thin 'butterfly skin' could be categorized as two groups: one with constant clear spacing of the air cavity of SBSwHR or SPS of SBSwPR (Figure 10.a)
and the other with variable clear spacing of air cavity or skin thickness of SPS (Figure 10.b and 10.c). The first group imitates the butterfly scale coverage (Figure 1); the second group imitates the moth scale coverage (Figure 4). The height of the air cavity is decreased in direction from the blade root BR to the blade tip BT ($h_{ftr} > h_{ftt}$, $h_{rtr} > h_{rtt}$, $h_{fbr} > h_{fbt}$, $h_{rbr} > h_{rbt}$), and in direction from the leading edge LE to the trailing edge TE ($h_{ftr} > h_{rtr}$, $h_{ftt} > h_{rtt}$, $h_{fbr} > h_{rbr}$, $h_{fbt} > h_{rbt}$); the clear spacing of the scale coverage which is attached to the lower blade surface LBS is more than one of the upper blade surface UBS ($h_{fbr} > h_{ftr}$, $h_{rbr} > h_{rtr}$, $h_{fbr} > h_{ftt}$, $h_{rbt} > h_{rtt}$) (Figure 10. c).

Experimental tests with porosity materials reveal that double porosity materials can achieve larger low frequency sound absorption compared to single porosity materials [100]. Consequently, UW (upper metal wall of SBSwHR) (Figure 10. a) could have double porosity structure: first porosity of the external wall is formed by rows of round perforation (Figure 10.a.1), secondly porosity of UW is formed by interparticle pores (Figure 10.a.2).

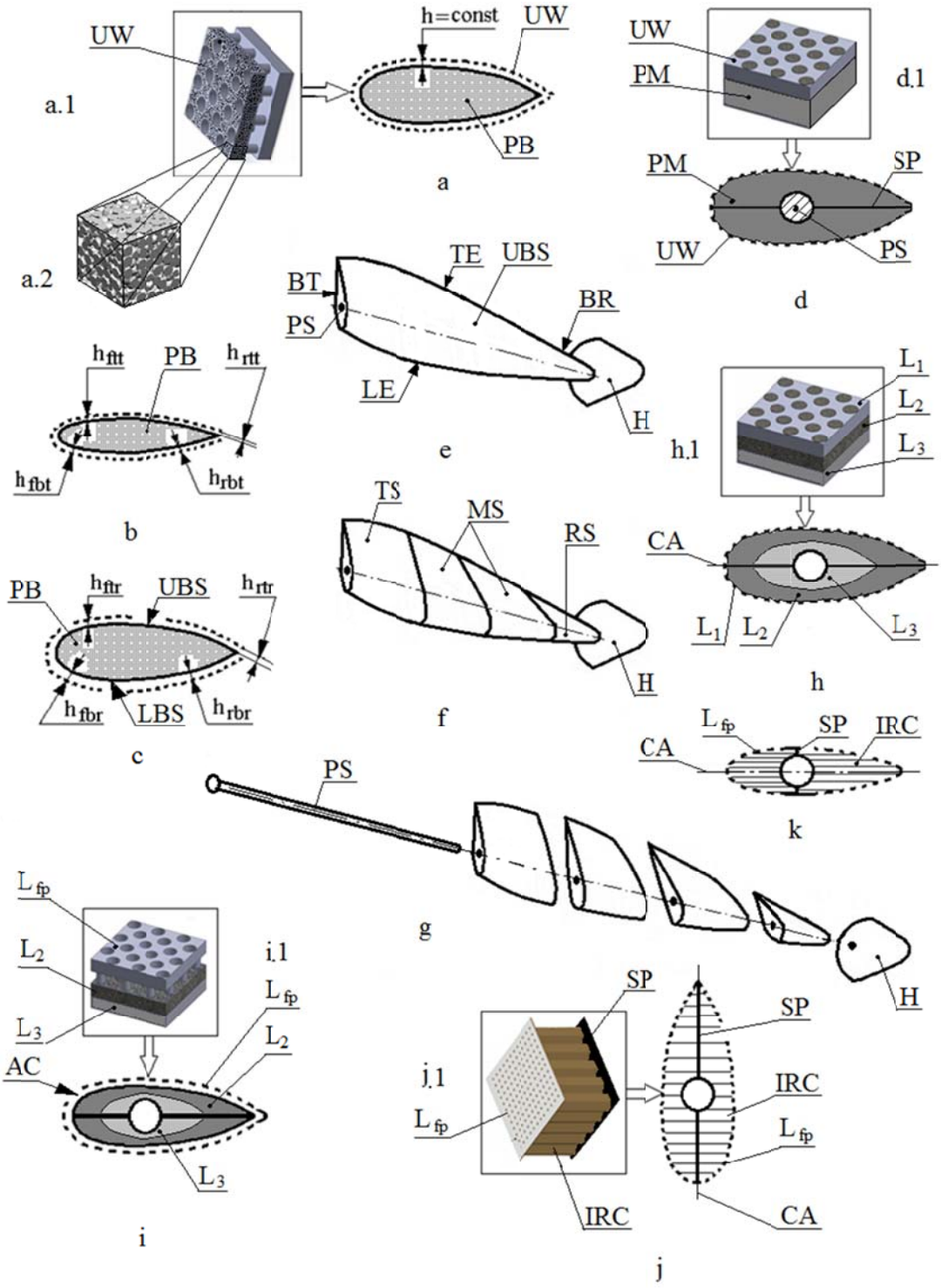

Figure 10 Different structural designs of 'butterfly acoustical skin' on parallel plans form propellers. a. propeller blade with constant clear spacing of BAS, a.1. a vertical cross-section of BAS with double porosity structure of upper metal wall, drawn in axonometric, a.2. second porosity structure of upper wall (3D computed tomography in axonometric plane), b. propeller root with variable air cavity of BAS, c. propeller tip with variable air cavity of BAS. d – thick type of BAS, d.1 – a vertical cross-section of the thick BAS, e. mono-segment type of BAS, f. propeller with multi-segment type of BAS in assembled condition, g. propeller with multi – segment type of BAS in

disassembled condition, h. sandwich structure of BAS, h. 1 vertical cross-section of the multi-layered group, drawn in axonometric, i. hybrid structure of BAS, i. 1 vertical cross-section of the hybrid structure of BAS, j. normal camber group of thick type BAS (the Figure is rotated 90 degrees counterclockwise about the center of the Figure), j. 1 vertical cross-section of the normal camber group of thick type BAS, drawn in axonometric, k. parallel camber group of thick type BAS, h_{ftt} – forward clear spacing of SBswHp (or thickness of SPS) on top of propeller tip, h_{fbt} – forward clear spacing of SBswHp (or thickness of SPS) on bottom of propeller tip, h_{ftr} – forward clear spacing of SBswHp (or thickness of SPS) on top of propeller root, h_{fbr} - forward clear spacing of SBswHp (or thickness of SPS) on bottom of propeller root, h_{rtt} – rear clear spacing of SBswHp (or thickness of SPS) on top of propeller tip, h_{rbt} – rear clear spacing of SBswHp (or thickness of SPS) on bottom of propeller tip, h_{rtr} – rear clear spacing of SBswHp (or thickness of SPS) on top of blade root, h_{rbr} – rear clear spacing of SBswHp (or thickness of SPS) on bottom of propeller root.

LE – leading edge, TE – trailing edge, BT – blade tip, BR – blade root, UBS – upper blade surface, LBS – lower blade surface, PB – propeller blade, L_{fp} – face porous layer, AC – air cavity, L_1, L_2 and L_3 – porous layers, CA – chord axes, TS –tip segment, MS – middle segment, RS – root segment, UW – upper metal wall of 'butterfly acoustical skin', PS – propeller spar, UBS – upper blade surface, PM – porous material, SP – solid partitions, H – propeller hub, IRC – internal resonant chamber.

It is well know, that the ability of porous material to absorb acoustic energy is increased in direct proportion to the thickness of a material [101 and 102]. But, if the thin skin thickness is significantly increases, it will cause an undesirable increase in the propeller overall dimensions and propeller weight. In contrast to it, the thick type of 'butterfly acoustical skin' is formed around the propeller spar (PS) and is affixed on the spar (Figure 10.d). UW of the 'butterfly skin' forms both the upper blade surface (UBS) (Figure 10.e) and the propeller blade shape. The space around the PS is filled with the porous material (PM). UW is supported from the inside with solid partitions (SP) and PM (Figure 10.d).

The thick 'butterfly acoustical skin' could also be classified as mono-segment type (Figure 10. e) and multi-segment type (Figure 10. f). First type of thick BAS is made as one-piece segment (Figure 10.e) and the second type is made with several 'butterfly acoustical skin' segments (Figure 10.f). Initially, these segments are manufactured, then they are dressed (more precisely, are strung) on the propeller spar, which, in the end, is attached to the propeller hub (H) (Figure 10.g). Since the porous structure has negative effect on the mechanical properties of a construction (the pores tend to decrease the mechanical strength [103], so the propeller spar PS and propeller blade PB (Figure 10) have a solid structure.

By analog with the scale coverage of the lepidopterans, the porous material PM of the thick BAS can be categorized as two groups: one – mono-layered – with uniform porosity (Figure 10.d), and the other – multi-layered (sandwich) – with differential porosity (Figure 10.h). The first group of thick skin imitates the butterfly scale coverage (ure. 1.c). The porous material of the second group has distinct layers with differential porosity. For example, Figure 10.h.1 shows the concept of thick BAS with three layers: L_1, L_2 and L_3, having different micro - configurations (Figure 10.h.1) (for example: cellular, fibrous or granular). The second group of thick BAS imitates the cabbage moth scale coverage (Figure 4).

Hybrid structure (Figure 10.i) of thick BAS could be used to increase the sound absorbing capabilities of the 'butterfly acoustical skin'. The hybrid structure is constructed with distinct regions of different materials. For example, Figure 10.i.1 shows concept of a hybrid structure with a face porous layer (L_{fp}), air cavity (AC) and two inner porous layers (L_2 and L_3). These porous layers and air cavity that in themselves would not be useful as an acoustic absorber could be incorporated as part of hybrid structure of 'butterfly acoustical skin' to yield an efficient acoustic absorber.

Another propeller noise reduction structure of ‘butterfly acoustical skin’ could be used. It is a chamber structure (Figure 10. j and 10. k). The chamber structure is constructed with a face porous layer (L_{fp}) and internal resonant chambers (IRC). L_{fp} forms the upper blade surface and the L_{fp} is supported from the inside with IRC and solid partitions (SP). By analogy with an acoustic line [84] and a soft vane [89] the chamber structure of ‘butterfly acoustical skin’ could be categorized as two groups: normal and parallel. The internal chambers or Helmholtz resonators of the first group are normal to the chord axes (CA) (Figure 10. j.1) and those of the second group are parallel to the chord axes (Figure 10.k). The first group of the chamber structure imitates the arrangement of moth appendages on the head vertex (Figure 4. d); the second group of the chamber structure imitates the arrangement of butterfly scales on insect wings.

By analogy with a structure of the scale coverage on the forewing of the cabbage moth (Figure 4), the structural design of the tip segment (TS) of 'butterfly acoustical skin' could be presented as a thin type (Figure 10.a) or as a parallel camber group of thick BAS (Figure 10.k); the design of either the middle segment (MS) could be presented as mono-layered group (Figure 10.d), or as a multi-layered one (Figure 10.h), or as a hybrid structure (Figure 10.i); and the design of root segment (RS) could be presented as a normal camber group of thick BAS (Figure 10.j).

'Butterfly acoustical skin' will become a very effective means to improve acoustic performances of the propeller-based propulsion systems. A higher acoustical performance of propeller blades with BAS can improve flying quality, safety, and comfort of passengers and residents of airport neighborhood. It can reduce detectability in military operations (detection of an aircraft with this propeller by an enemy’s passive acoustic system can be difficult). In addition to the aircraft, the butterfly skin could also be used in jet engines and in submarines.

5. Conclusion

The potential of the ‘butterfly acoustical skin’, as a new method of reduction aero acoustical noise for a quiet propeller, has been evaluated.

This topic is particularly relevant due to the increase of the propellers for civil and military purposes with multiple operational issues. The quietness and efficiency of the propulsive system are key aspects in the design of advanced aerial vehicles and very often can lead to the success or failure of a mission.

Attention was initially directed to this problem by observation of the porous scales and porous scale coverage of lepidopterans as well as other studies indicating the noise suppression of flying lepidopterans by wing appendages; the property of the moth coverage allows these insects to overcome bat’s attacks at night. These appendages are very small (size: 30 – 200 μm) and have a various porous structure. Many different micro – and nanostructures of the porous scales and many differences in details among various structures of the porous scale coverage of lepidonterans were discussed. I considered here only the porous scales of the butterflies *Papilio nireus*, *Nieris rapae, Deelias nigrina*, male *Callophrys rubi*, male *Polyommatus daphnis*, butterfly *Papilio palinurus* as well porous scale coverage of the cabbage moth, the moth of Saturniidae family and a moth of *Noctuoidea* family. The evolutionary history of lepidopterans and the properties of lepidopterans scale coverage were briefly described. Different methods of reducing aero acoustic noise of aircrafts were discussed.

The design of ‘butterfly acoustical skin’ with a hollow region imitates the cover hollow wing scale of the *Papilio nireus* butterfly. The design of ‘butterfly acoustical skin’ with a porous region imitates the cover hollow wing scale of the *Pieris rapae* butterfly, and from the cover hollow wing scale of the *Delieas nigrina* butterfly. The results illustrate the influence of ‘butterfly acoustical skin’ structure on the acoustic performances of two – bladed propeller. The studies show that the noise

reduction of a rotating propeller, at a Reynolds number of 200000, by smooth 'butterfly acoustical skin' with a porous region is 4 dB, and the noise reduction of a propeller by smooth 'butterfly acoustical skin' with a hollow region is 2 dB. The modification of acoustical effects on the rotating propeller with 'butterfly acoustical skin' was due both to an acoustic absorption, to a dissipation of turbulent energy, to a reducing influence on noise generated and to reducing the pressure difference.

Based on the method of reducing noise of lepidopterans both by porous structure of wing appendages and by porous structure of moth body coverage, which evolved for many million years through a natural selection, I show different designs of future 'butterfly acoustical skin', by analogy with a structure of scale and of scale coverage of lepidopterans.

It was determined in qualitative researches that the 'butterfly acoustical skin' influenced on the acoustic performances of two-bladed propeller. Other studies of 'butterfly skin' shoved that the skin increased the lift force and reduced the wing vibration. An experimental investigation of the effect of BAS on vibration and aerodynamic performances of propeller was not within the scope of this experiment. A full explanation, with different wind speeds and blade RPM, must await more detailed studies. But it does not seem unreasonable to suggest the possibility of some optimal BAS geometry and its structure to further augment thrust and reduce the noise and vibration of propeller.

Acknowledgements

I would like to thank my advisor Dr. Olga Bocharova–Messner for her comments. I thank the external reviewers for their constructive comments. The author would like to acknowledge the Zaporozhye Machine-Building Design Bureau for its collaboration.

References

[1] *Benyus, J. M. Biomimicry: Innovation Inspired by Nature (New York: William Morrow);* ***1997****; p. 320.*
[2] *Mascha, E. Uber die Schwungfedern. Zeitschrift fur wissenschaftliche Zoologie. 1903, 77, 606 – 551.*
[3] *Sarradj, E. A. Fast Signal Subspace Approach for the Determination of Absolute Levels from Phased Microphone Array Measurements. Journal of Sound and Vibration. 2010, 329, 1553 -1569.*
[4] *Graham, R. R. The Silent Flight of Owls. Journal of the Royal Aeronautical Society. 1934, 286, 837 – 843.*
[5] *Howe, M. Aerodynamic noise of a serrated trailing edge. Journal of Fluids and Structures. 1991, 5, 33–45.*
[6] *Howe, M. Noise produced by a sawtooth trailing edge. Journal of the Acoustical Society of America. 1991, 90(1), 482–487.*
[7] *Herr, M. & Dobrzynski, W. Experimental investigation in low-noise trailing edge design. AIAA Journal. 2005, 43(6), 1167–1175.*
[8] *Herr, M. Design criteria for low-noise trailing-edges. 13th AIAA/CEAS Aeroacoustics Conference. 2007. 2007-3470, 21–23 May.*
[9] *Geyer, T.; Sarradj, E. and Fritzsche, C. Measurement of the Noise Generation at the Trailing Edge of Porous Airfoils. Experiments in Fluids. 2010, 48(2), 291 – 308.*
[10] *Lian, C. and Zhuge, Y. Optimum Mix Design of Enhanced Permeable Concrete - an Experimental Investigation. Construction and Building Materials. 2010, 24, 2664-2571.*
[11] *Soderman, P. Aerodynamic effects of Leading Edge Serrations on a two dimensional Airfoil. NASA Technical Memorandum. TM X- 2643. 1972.*
[12] *Guidati, G.; Ostertag. J. and Wagner, S. Prediction and reduction of wind turbine noise: an overview of research activities in Europe. AIAA Paper 2000-0042, 2000.*
[13] *Simmons, J. A. and Vernon, J. A. Echolocation: discrimination of targets by the bat Eptesicus fuscus. J. Exp. Zoo. 1971, 176, 315–328.*
[14] *Simmons, J. A.; Lavender, W. A.; Lavender, B. A.; Doroshow, C. A.; Kiefer, S. W.; Livingston, R. and Scallet, A. C. Target structure and echo spectral discrimination by echolocating bats.* Science. *1974, 186,1130 – 1132.*
[15] *Schnitzler, H. U. Die ultraschall-ortungslaute der hufeisen-fledermause (Chiroptera – Rhinolophidae) in verschiedenen orientierungs-situationen.* Z. Vgl. Physiol. *1968, 57, 376–408.*
[16] *Kovalev, I. S. Acoustic properties of wing scaling in Noctuid Moth. Entomological Review.* ***2003****, 82 (2), 270 – 275.*

[17]Kovalev, I. S. and Brodsky, A. K. Of the role that elasticity and scales coating of the wings play in the flight stability of insects. Bulletin of the S. Petersburg State University. 1996, 3 (3), 3-7.
[18] Roeder, K. D. Echoes of ultrasonic pulses from flying moths. Biol. Bull. 1963, 124, 200 –210.
[19] Kovalev, I. S. Effect of the scales coverage of the moth gastropacha populifolia esper (Lepidoptera, lasiocampidae) on the reflection of the bat echolocation signal. Entomological Review. 2004, 83, 513 – 515.
[20] Ntelezos, A.; Guarato, F. and Windmill, J. F. C. The anti-bat strategy of ultrasound absorption: the wings of nocturnal moths (Bombycoidea: Saturniidae) absorb more ultrasound than the wings of diurnal moths (Chalcosiinae: Zygaenoidea: Zygaenidae), Biology Open. *2017, 6, 109 – 117.*
[21] Jinyao Zeng, Ning Xiang, Lei Jiang, Gareth Jones, Yongmei Zheng, Bingwan Liu, Shuyi Zhang. Moth Wing Scales Slightly Increase the Absorbance of Bat Echolocation Calls. PloS One. 6 : e27190.
[22] Zhiyuan Shen, Thomas R. Neil, Daniel Robert, Bruce W. Drinkwater, and Marc W. Holderied. Biomechanics of a moth scale at ultrasonic frequencies. Proceedings of the natural Academy of Sciences. 2018, 115:48, 12200-12205.
[23] Capinera, John L. Encyclopedia of Entomology. Butterflies and moths. 4, 2nd ed.: Springer, 2008; pp. 626–672.
[24]Brown. The book of butterflies, sphinxes and moths; illustrated by one hundred and forty-four engravings, coloured after nature; in three volumes, 1832.
[25] Ingram, A. L.; Parker, A. R. A review of the diversity and evolution of photonic structures in butterflies, incorporating the work of John Huxley (The Natural History Museum, London from 1961 to 1990). Phil. Trans. R. Soc. B. 2008, 363, 2465 – 2480.
[26] Weber, H. Lehrbuch der entomologie. Veslag Gustav Fischer. 1933, p. 728.
[28] Corkery RW, Tyrode EC. On the colour of wing scales in butterflies: iridescence and preferred orientation of single gyroid photonic crystals. Interface Focus. *2017, 7: 20160154, pp 1-16.*
[29] Schröder-Turk G.E., Wickham S., Averdunk H., Brink F., Fitz Gerald J.D., Poladian L., Large M.C.J., Hyde S.T. The chiral structure of porous chitin within the wing-scales of Callophrys rubi. Journal of Structural Biology. 2011, 174, pp. 290-295.
[30] Kükenthal, W. Handbuch der Zoologie/Handbook of Zoology. *2003.*
[31] Hooijdonk, E.; Vandenbem, C.; Berthier, S. and Vigneron, J. Bi-functional photonic structure in the (Papilionidae): modeling by scattering-matrix optical simulations. Opt. Express. 2012, 20, 22001 – 22011.
[32] Michielsen, K.; Stavenga, D. G. Gyroid cuticular structures in butterfly wing scales: biological photonic crystals. J. R. Soc. Interface. 2008, 5, 85–94.
[33] Morris, R. B. Iridescence from diffraction structures in the wing scales of Callophrys rubi, the Green Hairstreak. J. Entomol. (A). 1975, 49, 149–154.
[34] Stavenga, D. G.; Stowe, S.; Siebke, K.; Zeil, J. & Arikawa, K. Butterfly wing colours: scale beads make white pierid wings brighter. *Proc. R. Soc. B. 2004, 271, 1577–1584.*
[35] Lou, S.; Guo, X.; Fan, T and Zhang, D. Butterflies: inspiration for solar cells and sunlight water-splitting catalysts Energy. Environ. Sci. *2012, 11, 9195 – 9216.*
[36] Trzeciak, T. M.; Wilts, B. D.; Stavenga, D. G. and Vukusic, P. Variable multilayer reflection together with long-pass filtering pigment determines the wing coloration of papilionid butterflies of the nireusgroup. Opt. Express. 2012, 20, 8877 - 8890.
[37] Mille, C.; Tyrode, E. C. and Corkery, R. W. 3D titania photonic crystals replicated from gyroid structures in butterfly wing scales: approaching full band gaps at visible wavelengths. RSC Adv. 2013, 3, 109 – 117.
[38] Biró, L. P.; Bálint, Zs.; Kertész, K. et al. *Role of photonic-crystal-type structures in the thermal regulation of a Lycaenid butterfly sister species pair.* Phys. Rev. E. *2003, 67, 021907-1–7.*
[39] Tam, H. L.; Cheah, K. W.; Goh, D. and Goh, J. Iridescence and nano-structure differences in Papilio butterflies. Optical Materials Express. 2013, 3, 1087 – 1092.
[40] Kovalev, I. S. and Brodsky, A. K. Structure and some functional characteristics of the scale coverage in the cabbage moth Barathra brassicae L. Lepidoptera, Noctuidae. Entomological Review. 1996, 75 (3), 530 – 540.
[41] Kovalev, I. S. The Effect of 'Butterfly skin' with Rough Internal Surface *on the Performances of an Oscillating Airfoil, International Journal of Flow Control, 2014, 6, 125 – 140.*
[42] Hall, J. P. W.; Robbins, R. K. and Harvey, D. J. Extinction and biogeography in the Caribbean: new evidence from a fossil riodinid butterfly in Dominican amber. Proceedings of the Royal Society of London B. *2004, 271, 797 – 801.*
[43] Grimaldi, D. and Engel, M. S. Evolution of the Insects *(Cambridge University Press). 2005, p. 755.*
[44] Nachtigall, W. Die aerodinamische Funrtion der Schmetterlingsschuppen. Naturwissenschaften. 1965, 52 (9), 216 – 217.
[45] Kovalev, I. S. The Functional Role of the Hollow Region of the Butterfly Pyrameis atalanta (L.). Scale Journal of Bionic Engineering. 2008, 5, 224 – 230.
[46] Wasserthal, L. T. The role of butterfly wings in regulation of body temperature. Journal of Insect Physiology. 1975, 21, 1921 – 1930.

[47] Vukusic, P. and Sambles, J. R. Photonic structure in biology. Nature. 2003, 424, 852 – 855.
[48] Burghardt, F.; Knüttel, H.; Becker, M. and Fiedler, K, Flavonoid wing pigments increase attractiveness of female common blue (Polyommatus icarus) butterflies to mate-searching males. Naturwissenschaften. 2000, 87, 304 – 307.
[49] Brunton, C. and Majerus, M. Ultraviolet colours in butterflies: intra-or inter-specific communication. Pro. R. Soc. B. 1995, 260, 199 – 204.
[50] Mallet, J. and Singer, M. Individual selection, kin selection, and the shifting balance in the evolution of warning colours: the evidence from butterflies. Biol. J. Linn. Soc. 1987, 32, 337 – 350.
[51] Brakefield, P. and Liebert, T. Evolutionary dynamics of declining melanism in the peppered moth in the Netherlands. Proc. R. Soc. B. 2000, 267, 1953 – 1957.
[52]Kingsolver, J. and Watt, W. Thermoregulatory strategies in Colias butterflies: thermal stress and the limits to adaptation in temporally varying environments. Am. Nat. 1983, 12, 32 – 55.
[53] Srinivasarao, M. Nano-optics in the biological world: beetles, butterflies, birds, and moths. Chem. Rev. 1999, 99, 1935 – 1961.
[54] Nakano, R.; Skals, N.; Takanashi, T.; Surlykke, A.; Koike, T. et al. Moths produce extremely quiet ultrasonic courtship songs by rubbing specialized scales. Proc. Natl. Acad. Sci. USA. 2008, 105, 11812 – 11817.
[55] Eisner, T.; Alsop, R. and Ettershank, G. Adhesiveness of spider silk. Science. 1964, 146, 1058 – 1061.
[56] Sappington, T. W. and Showers, W. B. Reproductive maturity, mating status, and long-duration ßight behavior of Agrotis ipsilon (Lepidoptera: Noctuidae) and the conceptual misuse of the oogenesis-ßight syndrome by entomologists Environ. Entomol. 1992, 21, 677 – 688.
[57] Leishman, J. G. Principles of Helicopter Aerodynamics *(Cambridge aerospace series). 2006, p. 817.*
[58] Hubbard, H. H. Aeroacoustics of Flight Vehicles: Theory and Practice. NASA. 1991, 1, p. 610.
[59] Holmes, J. B.; Durham, H. M. and Tarry, E. S. Small Aircraft Transportation System Concept and Technologies. Journal of Aircraft. 2004, 41 (1), 26 – 35.
[60] Smith, S. W. The Scientist and Engineer's Guide to Digital Signal Processing. (California Technical Publishing). 1997, p. 643.
[61] Theodorsen, *T. and* Regler, *A. A. The* Problem of Noise Reduction with Reference *to Light Airplanes. NACA 1145, 1946.*
[62] Metzger, F. B. An Assessment of Propeller Aircraft Noise Reduction. Technology NASA. 1995, 198237.
[63]Mixson, J.; Greene, G. and Dempsey, T. Sources, Control and Effects of Noise From Aircraft Propellers and Rotors. NASA. 1981, 81971.
[64] Hoehne, V. O. and Luce, R. G. The Quieted Aircraft as a Military Tool. AIAA. 1969, Paper 792.
[65] Fulghum, A. D. Stealth Now. Aviation Week and Space Technology. 2005, 162, 13, p. 38.
[66]Farassat, F. and Succi, G. P. A review of propeller discrete frequency noise prediction technology with emphasis on two current methods for time domain calculations. Journal of Sound and Vibration. 1980, 71(3), 399-419.
[67]Brooks, T. F. and Schlinker, R. H. Progress in rotor broadband noise research. 1983, 7, 287–307.
[68]Magliozzi, B.; Hanson, D. B. and Amiet, R. K. Propeller and Propfan Noise. NASA . 1991, 1258.
[69]Nagel, A.; Levy, D. E. and Shepshelovich, M. Conceptual Aerodynamic Evolution of Mini/Micro UAV. 44th AIAA Aerospace Sciences Meeting and Exhibit AIAA. 2006, 1261.
[70] Sobieszczanski-Sobieski, J. and Haftka, R. T. Multidisciplinary Aerospace Design Optimization: Survey of Recent Developments. Structural Optimization. 1997, 14, 1 – 23.
[71] Hayden, R. and Chanaud, R. Foil structures with reduced sound generation. Us. Patent. 1974, 3853428.
[72] Chanaud, R. C. Noise reduction in propeller fans using porous blades at free-flow conditions. The Journal of the Acoustical Society of America. 1971, 51, 15 – 18.
[73]Chanaud, R.; Kong, N. and Sitterding, R. Experiments on porous blades as a means of reducing fan noise. The Journal of the Acoustical Society of America. 1976, 59, 564 – 575.
[74]Revell, J.; Kuntz, H.; Balena, F.; Horne, W.; Storms, B. and Dougherty, R. Trailing Edge Flap Noise Reduction by Porous Acoustic Treatment. 3rd AIAA/CEAS Aeroacoustics Conference. 1997, 1646.
[75]Lee, S. Effect of leading-edge porosity on blade-vortex interaction noise. AIAA. 1993, 0601.
[76]Khorrami, M. and Choudari, M. Application of Passive Porous Treatment to Slat Trailing Edge Noise. NASA. 2003, 212416.
[77]Khorrami, M. and Choudari, MA Novel Approach for Reducing Rotor Tip-Clearance Induced Noise in TurbofanEngines. 7th AIAA/CEAS Aeroacoustics Conference. 2001, 2148.
[78]Tinetti, A.; Kelly, J.; Thomas, R. and Bauer, S. Reduction of Wake-Stator Interaction Noise Using Passive Porosity. 40th AIAA Aerospace Sciences Meeting and Exhibit. 2002, 1036.
[79]Lockard, D. and Lilley, G. The Airframe Noise Reduction Challenge. NASA. 2004, 213013.
[80]Rackl, G.; Miller, G.; Guo, Y. and Yamamoto, K. Airframe Noise Studies - Review and Future Direction. NASA. 2005, 213767.

[81]Baines, W. D. and Peterson, E. G. An Investigation of Flow Through Screens. Transactions of the ASME. 1951, p. 36.
[82]Schubauer, G. B.; Spangenberg, W. G. and Klebanoff, P. S. Aerodynamic Characteristics of Damping Screens. NACA. 1950, 2001.
[83]Dannenberg, R. E.; Weiberg, J. A. and Gambucci, B. J. The Resistance to Airflow of Porous Materials Suitable for Boundary Layer Control Applications using Area Suction NACA. 1954, 3094.
[84]Jones, M. G.; Tracy, M. B.; Watson, W. R. and Parrott, T. L. Effects of liner geometry on acoustic impedance. 8th AIAA/CEAS Aeroacoustics Conference. 2002, 2446.
[85]Maa, D. Y. Theory and design of microperforated panel sound absorbing construction. Sci. Sin. 1975, 18. 55 – 71.
[86]Wood, R. M.; Banks, D. W. and Bauer, S. X. S. Assessment of Passive Porosity with Free and Fixed Separation on a Tangent Ogive Forebody. AIAA. 1992, 4494.
[87]Gillian, M. A. Computational Analysis of Drag Reduction and Buffet Alleviation on Viscous Transonic Flow over Porous Airfoils. AIAA. 1993, 3419.
[88]Bauer, S. X. S. and Hemsch, M. J. Alleviation of Side Force on Tangent-Ogive Forebodies Using Passive Porosity. AIAA. 1992, 2711.
[89]Jones, M.; Parrott, T.; Sutliff, D.; Hughes, C. Assessment of Soft Vane and Metal Foam Engine Noise Reduction Concepts. AIAA. 2009, 3142.
[90] Kovalev, I. From butterfly. LAMBERT Academic Publishing. 2017, p. 38.
[91]Roger, M. and Moreau, S. Broadband self-noise from loaded fan blades. AIAA Journal. 2004, 42(3), 536–544.
[92]Pagano, M.; Barbarino, D.; Casalino, P. and Federico, L. Tonal and Broadband Noise Calculations for Aeroacoustic Optimization of Propeller Blades in a Pusher Configuration. Journal of Aircraft. 2010, 47(3).
[93]Sinibaldi, G. and Marino, L. Experimental analysis on the noise of propellers for small UAV. Applied Acoustics. 2013, 74, 79 – 88.
[94]Pechan, T. and Sescu, A. Experimental study of noise emitted by propeller's *surface imperfections. Applied Acoustics. 2015, 92, 12 – 17.*
[95]Hamakawa, H.; Hosokai, K.; Adachi, T.; Kurihara, E. Aerodynamic Sound radiated from Two-Dimensional Airfoil with Local Porous Material. Open Journal of Fluid Dynamics. 2013, 3, 55 – 60.
[96] Flumerfelt, J. F. Aluminum powder metallurgy processing. Retrospective Theses and Dissertations. 1998, 11918.
[97]Sarradj, E. and Geyer, T. Noise generation by porous airfoils. 13th AIAA/CEAS aeroacoustics conference. 2007, 3719.
[98]Allard, J. F. Propagation of Sound in Porous Media: Modelling Sound Absorbing Materials. John Wiley & Sons. 2009, p. 351.
[99]Crocker, M. J. and Arenas, J. P. Use of Sound-Absorbing Materials. John Wiley and Sons. 2007, 696-713.
[100]Venegas, R. and Umnova, O. Acoustical properties of double porosity granular materials. The Journal of the Acoustical Society of America. 2011, 130 (5), 2765 – 2776.
[101]Kuczmarski, M. A. and Johnston, J. C. Acoustic Absorption in Porous Materials. NASA. 2011, 216995.
[102]Cox T.J., D'Antonio P. Acoustic absorbers and diffusers: theory, design and application. Oxon: Taylor & Francis Group. 2009, p. 476.
[103]Mia, X. and Sun, D. Graded/gradient porous biomaterials. Materials. 2010, 3, 26 – 47.